

. SCUOLA INTERNAZIONALE SUPERIORE DI STUDI AVANZATI

SISSA Digital Library

Afferent Input Induced by Rhythmic Limb Movement Modulates Spinal Neuronal Circuits in an Innovative Robotic In Vitro Preparation

Original
Afferent Input Induced by Rhythmic Limb Movement Modulates Spinal Neuronal Circuits in an Innovative Robotic In Vitro Preparation / Dingu, N., Deumens, R., Taccola, G.. - In: NEUROSCIENCE. - ISSN 0306-4522. - 394:(2018), pp. 44-59. [10.1016/j.neuroscience.2018.10.016]

Availability:
This version is available at: 20.500.11767/88234 since: 2019-03-18T08:35:21Z

Publisher:

Published
DOI:10.1016/j.neuroscience.2018.10.016

Terms of use:

Testo definito dall'ateneo relativo alle clausole di concessione d'uso

Publisher copyright
Elsevier

This version is available for education and non-commercial purposes.

note finali coverpage

(Article begins on next page)

26 November 2026

Afferent input induced by rhythmic limb movement modulates spinal neuronal circuits in an innovative robotic *in vitro* preparation

Nejada Dingu[a,b], Ronald Deumens[c], Giuliano Taccola[a,b]

[a]Neuroscience Department, International School for Advanced Studies (SISSA); [b]SPINAL (Spinal Person Injury Neurorehabilitation Applied Laboratory), Istituto di Medicina Fisica e Riabilitazione (IMFR), via Gervasutta 48, Udine (UD) Italy; [c]Institute of Neuroscience, Université catholique de Louvain, Av. Hippocrate 54, Brussels, Belgium.

Corresponding author: Dr. Giuliano Taccola, via Bonomea 265, Trieste, (TS) Italy; taccola@sissa.it.

Running title: passive exercise on spinal circuits

Keywords: spinal cord, locomotor patterns, motoneuron, dorsal afferents

Abbreviations

5-HT: 5-hydroxytryptamine, serotonin

AMPA: α-amino-3-hydroxy-5-methyl-4-isoxazolepropionic acid

ANOVA: analysis of variance

BIKE: Bipedal Induced Kinetic Exercise

CAP: compound action potential

CC: current clamp

CCF: cross-correlation function

CPG: central pattern generator

DR: dorsal root

DRDRP: dorsal root – dorsal root potential

DRVRP: dorsal root – ventral root potential

FFT: fast Fourier transform

FL: fictive locomotion

GABA: γ-aminobutyric acid

I-V: current-voltage

l: left

L: lumbar

NMDA: N-methyl-D-aspartate

P: postnatal

r: right

R_m: membrane resistance

RMS: root mean square

SCI: spinal cord injury

SD: standard deviation

sPSC: spontaneous post-synaptic current

T: thoracic

Th: threshold

VC: voltage clamp

V_m: membrane potential

V_{off}: offset voltage

VR: ventral root

Afferent input induced by rhythmic limb movements modulates spinal neuronal circuits in an innovative robotic *in vitro* preparation

Nejada Dingu, Ronald Deumens, Giuliano Taccola

Abstract

Locomotor patterns are mainly modulated by afferent feedback, but its actual contribution to spinal network activity during continuous passive limb training is still unexplored. To unveil this issue, we devised a robotic *in vitro* setup (Bipedal Induced Kinetic Exercise, BIKE) to induce passive pedaling, while simultaneously recording low-noise ventral and dorsal root (VR and DR) potentials in isolated neonatal rat spinal cords with hindlimbs attached. As a result, BIKE evoked rhythmic afferent volleys from DRs, reminiscent of pedaling speed. During BIKE, spontaneous VR activity remained unchanged, while a DR rhythmic component paired the pedaling pace. Moreover, BIKE onset rarely elicited brief episodes of fictive locomotion (FL) and, when trains of electrical pulses were simultaneously applied to a DR, it increased the amplitude, but not the number, of FL cycles. When BIKE was switched off after a 30-minute training, the number of electrically-induced FL oscillations was transitorily facilitated, without affecting VR reflexes nor DR potentials. However, 90-minutes of BIKE no longer facilitated FL, but strongly depressed area of VR reflexes and stably increased antidromic DR discharges. Patch clamp recordings from single motoneurons after 90-minute sessions indicated an increased frequency of both fast- and slow-decaying synaptic input to motoneurons. In conclusion, hindlimb rhythmic and alternated pedaling of different durations affects distinct dorsal and ventral spinal networks by modulating excitatory and inhibitory input to motoneurons. These results suggest defining new parameters for effective neurorehabilitation that better exploits spinal circuit activity.

Introduction

In the spinal cord, dedicated neuronal networks, known as Central Pattern Generators (CPGs), drive limb locomotion (Kiehn, 2006), as demonstrated by the alternating hindlimb movements induced by neurochemicals in the *in vitro* isolated neonatal spinal cord with legs attached (Kiehn and Kjaerulff, 1996; Klein and Tresch, 2010).

The CPG-driven movement of limbs stretches muscles and joint capsules and activates cutaneous receptors to generate an afferent feedback to the spinal cord (Loeb et al., 1977). Afferent feedback is crucial to modulate sensory-motor processing (Mandadi and Whelan, 2009; Mandadi et al., 2013; Sirois et al., 2013) and locomotor patterns (Hayes et al., 2009; Brumley et al., 2017). Indeed, locomotor patterns induced by neurochemicals disappear when afferent inputs are removed from a neonatal rat spinal cord preparations with limbs attached (Acevedo and Diaz-Rios, 2013). On the other hand, protocols of electrical stimulation applied to dorsal afferents elicit an epoch of locomotor-like cycles (Marchetti et al., 2001; Taccola, 2011; Dose and Taccola, 2016; Dose et al., 2016) and increase spontaneous activity of dorsal horn networks when repeatedly supplied (Dingu et al., 2016).

In clinics, the continuous flow of afferent input determined by sessions of repetitive and alternated limb movement facilitate the re-expression of locomotor patterns after a spinal lesion, probably because of the consequent plastic changes occurring in spared spinal circuits (Dietz and Fouad, 2014). Likewise, in preclinical models, increased expression of genes involved in motoneuronal plasticity (Joseph et al., 2012; Keeler et al., 2012; Chopek et al., 2015) and restored tuned balance between inhibitory and excitatory synaptic boutons to motoneurons (Ichiyama et al., 2011) were observed with alternating and passive hindlimb mobilization, as well as following activity-based interventions, such as passive cycling (Chopek et al., 2014; Côté et al., 2014).

This evidence confirms that afferent input triggers locomotor-like cycles, but it remains unclear how the afferent feedback evoked by the continuous mobilization of limbs modulates the ongoing activity of dorsal sensory-related and ventral motor-related spinal networks. It also needs to be determined whether a different duration of passive exercise can selectively modulate distinct spinal networks and extend its functional effects on spinal circuits even after session ending. Our hypothesis is that CPG-driven locomotor patterns are facilitated by afferent input generated during and after alternating leg movements. This study explores how the afferent input evoked by repetitive, passive alternating movements of hindlimbs modulates patterns generated by spinal networks, and how exercise sessions of different duration affect distinct spinal circuits.

We adopted an innovative robotic model that permits recording ventral and dorsal root (VR and DR) activity during passive pedaling in a neonatal preparation of isolated spinal cord with legs attached. Although immature, this preparation can extend understanding of neuromotor system organization in humans, as well as of basic mechanisms of clinical rehabilitation, since many "building blocks" of the mammalian spinal circuitry are already present at birth (Getting, 1989; Stein, 1995; Nishimaru and Kudo, 2000). In neonatal isolated cords, rhythmic activity of ventral locomotor networks arises as epochs of electrical discharges alternating among homosegmental left and right VRs (Fictive Locomotion, FL; Juvin et al., 2007, Nistri et al., 2010). On the other hand, activity of dorsal sensory circuits is probed with monitoring spontaneous rhythmic antidromic discharges recorded synchronously among DRs (Vinay et al., 1999).

The question addressed by the present paper consists in the key physiological mechanisms driving spinal processing of afferent input, as elicited by passive limb mobilization. This issue is at the base of numerous rehabilitative techniques, which are currently being improved by exploiting passive and robotic walking for alleviating neuropathic pain and facilitating recovery of function in people with spinal cord injury (Harkema et al., 2012; Hubli and Dietz, 2013; Dugan and Sagen, 2015).

Experimental Procedures

In vitro *preparations of neonatal rat spinal cord and nerves*

All procedures were approved by the International School for Advanced Studies (SISSA) ethics committee and are in accordance with the guidelines of the National Institutes of Health (NIH) and with the Italian Animal Welfare Act 24/3/2014 n. 26 implementing the European Union directive on animal experimentation (2010/63/EU). Experiments were performed on preparations of isolated thoraco-sacral (from T3-4 to *cauda equina*) spinal cord with hindlimbs attached, obtained from neonatal Wistar rats at postnatal (P) days 0–4. All efforts were made to minimize the number and suffering of animals used for experiments. Spinal roots were bilaterally dissected from high thoracic spinal levels to the second lumbar segment (L2) included, leaving all spinal segments below L2 (from L3 on) ventrally and dorsally connected to the periphery. In a subset of experiments, a mechanical compression of the hindpaw was performed to elicit the corresponding afferent feedback from lumbar DRs. All preparations were placed in a recording chamber continuously superfused (5 mL/min) with oxygenated (95% O_2 – 5% CO_2) Krebs solution containing (in mM): 113 NaCl, 4.5 KCl, 1 $MgCl_2 7H_2O$, 2 $CaCl_2$, 1 NaH_2PO_4, 25 $NaHCO_3$ and 11 glucose, pH 7.4.

A new device to induce passive training

We designed and created a novel device, named BIKE (Bipedal Induced Kinetic Exercise), to induce passive training in the isolated spinal cord with legs attached (Fig. 1 A). The preparation was placed in the recording chamber (maintained at room temperature, 23-25 °C) using acrylic glue to attach the hindpaws to the pedals and to position the legs above the bath (Fig. 1 B). In this position, pedal rotation produced a maximal knee excursions of approximately 140 to 180 degrees (Fig. 1 C). BIKE was connected to a stabilized power supply (K.E.R.T., Treviso, Italy), to allow an adaptable speed of rotation. The design of BIKE carefully considered grounding and shielding from noise, by adopting a brushless DC electric motor. Movement was set at an operative speed of 30-35 cycles/min (pedaling frequency = 0.5 Hz) to mimic the standard periodicity of a pharmacologically-induced locomotor-like pattern by NMDA (5 μM) and 5HT (10 μM; Dose and Taccola, 2012; Taccola et al., 2012). To verify that recordings remained stable even after a long maintenance of preparations in experimental conditions, sham experiments were performed by keeping the spinal cord with legs attached in Krebs solution with hindpaws firmly fixed to BIKE pedals while the device was switched off. The preparation underwent the same stimulation and recording protocols and at the same time points used on BIKE samples for testing spinal network activity (Fig. 1 A).

Nerve recordings

All recordings were taken after 40–60 min of steady state period to normalize the specimen from any post-surgical depressions. In Fig. 1 A are summarized protocols of extracellular recordings and stimulations. Using tight-fitting monopolar suction electrodes, simultaneous DC-coupled recordings were extracellularly obtained from whole L2 ventral roots (VRs) right (r) and left (l) and from the whole dorsal root (DR), either L1 or L2. Recordings of DR potentials from L5 were performed *en passant* by applying a negative pressure through a pipette close to the root surface. To isolate the sole contribution of the sensory input elicited in the periphery by passive limb mobilization, in a sub group of preparations, all spinal nerves were bilaterally transected, the spinal cord removed and distal stumps suctioned in glass pipette electrodes connected to an AC-coupled amplifier. Afterwards, a pair of hooked needle electrodes (Sei s.r.l., Padova, Italy) was used to record compound action potentials (CAPs) from one sciatic nerve (exposed proximally to its trifurcation) and dorsal afferent nerves following electrical stimulation of the territory of the hindpaw innervated by the sural nerve.

AC- and DC-coupled recordings were acquired with a differential amplifier (DP-304®, Warner Instruments, CT, USA; low-pass filter = 10 Hz, high-pass filter = 0.1 Hz, gain = 1000) at a sampling rate of 10 or 50 kHz, digitized (Digidata 1440®, Molecular Devices Corporation, Downingtown, PA, USA), visualized real time with the software Clampex 10.3® (Molecular Devices Corporation, Downingtown, PA, USA) and stored on a PC for off-line analysis. A bipolar suction electrode connected to a programmable stimulator (STG4002®, Multichannel Systems, Reutlingen, Germany) was used to deliver single or repeated electrical pulses to a DR (either l or r T13 - L2). Intensity of stimulation was determined in terms of threshold (Th), namely the lowest stimulus intensity capable of eliciting an appreciable response from the homologous VR for determining DRVRPs and from the homosegmental DRs for DRDRPs (Bracci et al., 1996a). Overall, the mean value of Th was 27.40 ± 18.35 µA. Responses were evoked by delivering single rectangular pulses (duration = 0.1 ms; intensity = 94.69 ± 42.56 µA, 3.15 ± 0.67 x Th) every 50 seconds. Episodes of fictive locomotion (FL) were induced by trains of electrical stimuli (120 rectangular pulses; frequency = 2 Hz; duration = 0.1 ms) delivered every 3 minutes to a DR at suprathreshold intensity (58.82 ± 35.80 µA, 2.07 ± 0.58 x Th). Single rectangular pulses (duration = 5 ms) were delivered every 50 seconds to the territory of the hindpaw innervated by the sural nerve, using STG4002® stimulator (Multichannel Systems, Reutlingen, Germany). Since the stimulating electrode around the nerve was kept out of the electrolyte solution, high impedance was overcome by applying an increased current (intensity = 16 mA; 4 x Th for eliciting an orthodromic CAP).

Parameters of spinal network activity

Afferent volleys on DRs were quantified using Clampex 10.3® (Molecular Devices Corporation, Downingtown, PA, USA) during off-line analysis. A template of incoming events was generated for each dorsal afferent nerve and used for the selection of discharges from the same nerve. Spontaneous activity was quantified in terms of power spectrum magnitude and expressed as Root Mean Square (RMS; Deumens et al., 2013). Briefly, Fast Fourier Transform (FFT) analysis decomposed fixed-length time windows (10, 20 or 90 minutes) into a number of discrete frequencies and their power distribution was measured with Clampex 10.3® (Molecular Devices Corporation, Downingtown, PA, USA). Analysis adopted a default rectangular windowing function, with data segments not overlapping, window length set at the largest value fitting within the data segments to be processed and the first spectral bin of the periodogram excluded from RMS measurements. The magnitude of the resulting spectrum is the summed power of all rhythm frequencies. This statistical tool

quantifies any increase in frequency and/or amplitude of spontaneous activity, expressed as a complex rhythm composed of multiple harmonics.

Ventral reflexes and electrically-evoked antidromic activity were assessed through series of single electrical stimuli delivered to a DR in pre-BIKE control, during training and after 30- and 90-minute BIKE sessions. At least 10 consecutive reflex responses were simultaneously recorded from one DR (dorsal root - dorsal root potentials, DRDRPs) and from one VR (dorsal root - ventral root potentials, DRVRPs; Kerkut and Bagust, 1995). Samples of equal duration were collected at each different time point. For analysis, multiple sweeps were averaged and the mean peak amplitude and area were quantified.

Alternating activity of the left and right VRs is indicative of a CPG-driven locomotor pattern (Fictive Locomotion, FL; Juvin et al., 2007). A FL oscillation is defined as a period of sustained membrane depolarizations remaining above a preset threshold (usually 5 times the standard deviation of baseline noise) for more than 400 ms (Bracci et al., 1996b). To determine the correlation between left and right VR activity, Cross-Correlation Function (CCF) was computed using Clampfit 10.3® software (Molecular Devices Corporation, PA, USA). A CCF > 0.5 at lag 0 correlation indicates that two roots are synchronous, while a CCF < - 0.5 shows full alternation.

Patch clamp recordings

Sacrolumbar cords were completely isolated from the leg-attached preparation. The dorsal surface of the cord was glued to an adjustable and articulated plastic support and bent at the level of upper sacral segments in a perpendicular upright position, by means of a Sylgard® 184 silicone elastomer cube (Dow Corning Corporation, Auburn, MI, USA), with the caudal cord facing upwards (Fig. 8 A). A horizontal section was cut at lumbar (L) 4-5 spinal segments using a vibratome (Leica VT 1000 S, Leica Biosystems) to remove the caudal lumbosacral segments. This upside-down configuration allows patch clamp recordings from spinal motoneurons (Fig. 8 A), still keeping intact the segments where the locomotor networks are mainly localized (Kjaerulff et al., 1994; Kremer and Lev-Tov, 1997; Cowley and Schmidt, 1997). The entire procedure from the end of BIKE to onset of patch clamp recordings requires at least 45 min. Patch clamp recordings in whole-cell configuration were made on L4-L5 motoneurons from isolated spinal cords, either after training (30, 90 min) or in experiments in which spinal cords were kept still in the BIKE recording chamber without BIKE functioning, for the same time interval as the trained cords (sham). Note that experimental protocols adopted in sham preparations were identical to BIKE-trained

preparations, with the exception that shams did not undergo any passive cycling. Recordings were performed in both voltage clamp (VC) and current clamp (CC) modes. Up-right bent spinal cords were continuously superfused with oxygenated Krebs solution (flow rate = 7 ml/min), illuminated by a far-red-emitting optical fiber (Scientifica Ltd, Uckfield, UK) and visualized through two switchable objectives (4x and 40x; Olympus, Tokyo, Japan) of an infrared video camera (Olympus U-TV1x-2, Tokyo, Japan) connected to the monitor through a C-mount adapter (Olympus U-CMAD3, Tokyo, Japan). Firstly, motoneurons were visually identified in the ventral horn (Rexed laminae VIII – IX) based on their morphology (21-25 μm diameter and one or two large processes; Fulton and Walton, 1986; Cifra et al., 2012) and location (close to the VR, in an area corresponding to the Rexed's lamina IX; Molander et al., 1984). Once patched, their functional identity was confirmed by the appearance of antidromic action potentials in response to electrical stimulation of the corresponding VR. Recordings were obtained using borosilicate pipettes with a mean resistance of 6.07 ± 2.08 MΩ and filled with a solution containing (in mM): 120 K gluconate, 20 KCl, 10 HEPES, 10 EGTA, 2 $MgCl_2$, 2 Na_2ATP, adjusted to pH 7.3 with KOH (Fabbro et al., 2012). Series resistance (lower than 18 MΩ) was monitored throughout the experiment at specific time points and was not compensated. Cells were discarded if series resistance was higher than 25 MΩ and if it varied more than 20% of the initial value (Tartas et al., 2010; Bouhadfane et al., 2013). Liquid junction potential in our experimental conditions was equal to 12.8 mV (Barry, 1994) and all membrane potential values were corrected. Electrophysiological responses were amplified using a differential amplifier (ELC-03XS Amplifier, npi electronic GmbH, Tamm, Germany), digitized by Digidata 1440® (Molecular Devices Corporation, Downingtown, PA, USA) and visualized in real time with Clampex 10.3® (Molecular Devices Corporation, Downingtown, PA, USA). Data were acquired at a sampling rate of 10 kHz and subsequently analyzed off-line.

Parameters of motoneuronal activity

Synaptic activity to lumbar motoneurons was recorded in VC mode, keeping cells clamped at -60 mV. Spontaneous post-synaptic currents (sPSCs) were selected using templates and, based on their decay time, classified as fast- (τ = 5.43 ± 1.17 ms) and slow-decaying currents (τ = 20.10 ± 6.61 ms). Kinetic analysis was adopted to dissect out the following parameters: current frequency (Hz), peak amplitude (pA), time of peak (ms), area (pA * ms), half-width (ms), rise time (ms), rise slope (pA/ms), decay time (ms) and decay slope (pA/ms). Main kinetic properties of fast and slow sPSCs were calculated with Clampex 10.3® (Molecular

Devices Corporation, Downingtown, PA, USA). In addition, discrimination between fast glutamate-related currents and slow GABA/glycine-related currents was obtained by performing patch clamp recordings at different holding potentials. Holding potential was first equaled to the reversal potential for Cl^- to abolish GABA/glycine currents and to observe only glutamatergic PSCs. Similarly, the holding potential was then matched with the reversal potential for Na^+/K^+ cations to zero AMPA receptors contributions and to consider only chloride currents. Resting membrane potential (V_m = -82.90 ± 7.19 mV) of motoneurons was determined in CC mode without injecting any holding current (I = 0 nA). Afterwards, increasing steps of current were injected and membrane resistance (R_m) was calculated as the slope of the current-voltage (I-V) curve, which was linear in the interval considered. All membrane potentials were corrected for offset voltage (V_{off}), as obtained by raising the electrode from the cell at the end of each recording.

Statistical analysis

Data are expressed as mean ± SD. "n" indicates the number of preparations, while "n_{cells}" represents the number of recorded motoneurons. Normality and equal variance tests were used to determine appropriateness of parametric versus nonparametric comparisons. All parametric values were analyzed using Student's t-test (paired or unpaired) to compare two groups of data, or with one-way repeated measures ANOVA for more than two groups. Nonparametric comparisons were performed using Mann-Whitney rank sum test (unpaired) and Wilcoxon signed rank test (paired) for two groups, and with Friedman repeated measures ANOVA on ranks for multiple comparisons. Multiple comparisons were followed by a post hoc test versus control (Bonferroni t-test). Statistical analysis was performed using SigmaStat® 3.5 software (Systat Software Inc, San Jose, CA, USA). Results were considered significant when $P < 0.05$.

Results

BIKE generates real alternating hindlimb movement in vitro

We created a robotic device, named BIKE (Fig. 1 B), to allow stable recordings during passive hindlimb movement *in vitro*. Once a leg-attached isolated spinal cord preparation was placed in the recording chamber and hindpaws were fixed to the pedals, BIKE passively and alternatively propelled limbs (Fig. 1 C). BIKE was created with a unique low-noise design that abolishes electrical interference, as confirmed by the lack of artifacts during BIKE functioning (Fig. 1 D, E). In addition, no electrical nor mechanical interferences due to the

rotor engine or pedaling limb motion were detected by the probe electrode filled with Krebs solution placed close to the recorded spinal roots (Fig. 1 E). Indeed, from the spectral analysis of the background noise detected during BIKE, the rhythmic component of the main frequency of pedaling (0.5 Hz) was absent (Fig. 1 F).

To confirm persistence of consistent baseline recordings, in exemplar sham experiments, VR and DR traces were acquired and the spontaneous activity was calculated in 20-min bin intervals (Fig. 2). Power spectrum magnitude, expressed as RMS, remained consistent for more than three hours, confirming that the leg-attached isolated spinal cord provides stable long-term baseline values of the spontaneous activity recorded from DRs (Fig. 2 C; $F_{(9, 18)}$ = 0.849, P = 0.584, one-way repeated measures ANOVA, n = 3) and VRs (Fig. 2 D; $F_{(9, 18)}$ = 1.014, P = 0.465, one-way repeated measures ANOVA, n = 3).

BIKE evokes afferent input

BIKE can thus be used for testing whether passive hindlimb movement *in vitro* evokes a sensory feedback on the spinal cord. We faced this hypothesis using *en passant* AC-coupled nerve recordings from the whole DRlL5 (left L5 DR) in the isolated spinal cord with hindlimbs attached, during pre-BIKE control (90-minute), BIKE training and post-BIKE resting phases (Fig. 3 A). Exemplar traces highlight an increase of events from 10659 during pre-BIKE control to 12411 during BIKE, and the return to pre-BIKE control values with post-BIKE rest (9057; Fig. 3 A). Pooled experiments show an average increase of discharges during passive pedaling (138.11 ± 30.65 % of pre-BIKE control), an effect that waned in the following post-BIKE resting phase (110.70 ± 36.39 % of pre-BIKE control; $\chi^2_{(2)}$ = 3.000, P = 0.500, Friedman repeated measures ANOVA on ranks). To characterize the pattern of afferent discharges, Fast Fourier Transform (FFT) analysis was performed. During BIKE, a main rhythmic frequency component at 0.5 Hz appeared, which was absent both during pre-BIKE control (left) and after BIKE termination (right, Fig. 3 B). This rhythmic component at 0.5 Hz was not an electrical interference produced by BIKE functioning, since it was not detected by the probe electrode measuring bath polarization during pedaling (Fig. 1 E, F). Thus, during BIKE, a rhythmic component is elicited from afferents, pairing the frequency of passive limb movement. This rhythm had small amplitude and became appreciable only when magnified, as it was otherwise covered by the baseline background noise (Fig. 3 C).

Next, we wanted to isolate the sole contribution of sensory input with respect to antidromic discharges from dorsal horns. Thus, in a sub group of preparations (data not shown), we bilaterally transected spinal roots and removed the cord from the bath, with dorsal nerves still

connected to hindlimbs. Then, the distal stump of DRL5 was suctioned in glass pipette electrodes connected to an AC-coupled amplifier. In these experiments, the number of events recorded during BIKE was more than double the pre-BIKE control values (218.05 ± 65.81 %, W = 21, P = 0.031, Wilcoxon signed rank test, n = 6).

To exclude any bias due to a possible damage of afferent pathways, we defined a random sample of preparations, where each hind paw was peripherally stimulated to record afferent discharges from dorsal nerves (Fig 4). Orthodromic activity was recorded from DRlL4 during mechanical compression of the left hindpaw (an almost eight-fold frequency increase with respect to pre-compression control; see AC-coupled traces and raster plots in Fig. 4 A), as highlighted by the magnification of selected events in Fig. 4 B. Moreover, in another subset of experiments (Fig. 4 C), electrical stimulation of the skin innervated by the sural nerve evoked responses from the sciatic nerve and, with a higher latency, from spinal afferent nerves L4 and L5 (Fig. 4 D), demonstrating that afferent pathways still convey input from periphery to the dorsal spinal cord.

BIKE onset does not usually elicit FL per se, nor does it vary the number of oscillations of an ongoing FL.

To verify the effects of passive movement on rhythmic patterns generated by the locomotor CPG, we investigated whether BIKE functioning elicits spontaneous locomotor-like oscillations from VRs. In 85% of experiments (52/61), no FL was evoked during pedaling. In the remaining preparations (9/61), only a brief episode of spontaneous left-right alternating oscillations (0.55 ± 0.11 mV; 5 ± 3 cycles; data not shown) temporarily appeared when BIKE was switched on. Likewise, during 90 mins of BIKE (Fig. 5 A), we derived in DC mode a spontaneous tonic activity from VRs, with sporadic bursts provided of few superimposed oscillations with poor phase coupling (Fig. 5 B, C), as confirmed by CCF analysis performed on top of bursts (Fig. 5 D, E). In more details, the CCF at 0 lag for the first burst (B, D) shows a positive peak (0.18) for synchronous superimposed oscillations. On the other hand, the second event (C, E) at 0 lag depicts a negative CCF peak (-0.27), pointing out some alternating activity, albeit below the cutoff value (-0.5) for a full VR alternation, caused by the irregular rhythm. Spectral analysis of the spontaneous rhythmic activity (Fig. 5 A) at different time intervals during a 90 min BIKE session indicated that BIKE does not affect the spontaneous VR rhythmic pattern (Fig. 5 F; $\chi^2_{(6)} = 5.571$, P = 0.473, Friedman repeated measures ANOVA on ranks, n = 9).

Although BIKE onset only rarely elicited episodes of FL on its own, we explored whether BIKE still facilitates FL episodes evoked by electrical stimulation. We thus analyzed the rhythmic, alternating activity of l and r VRs when applying a train of rectangular pulses (2 Hz, 120 to 180 stimuli, 1.92 ± 0.38 Th) to different DRs (from DRT13 to DRL2). During pedaling, the addition of a train of electrical pulses did not change the number of FL oscillations (108.93 ± 19.06 % of pre-BIKE control; W = -1, P = 1.000, Wilcoxon signed rank test, n = 5) nor the cumulative depolarization peak (102.46 ± 3.83 % of pre-BIKE control; $t_{(4)}$ = -1.508, P = 0.206, paired t-test, n = 5). However, during pedaling, the amplitude of FL oscillations consistently increased (104.44 ± 3.55 % of pre-BIKE control) without any relation to either cycling phase or pulse occurrence. This mild modulatory action over the electrically-evoked FL faded away after BIKE termination ($F_{(2, 8)}$ = 7.433, P = 0.015, one-way repeated measures ANOVA, n = 5).

Different durations of BIKE application affect locomotor spinal circuits in a nonlinear manner

To test whether a protracted passive limb exercise could facilitate the locomotor pattern in the post-BIKE resting phase, 2 Hz trains of pulses were delivered before and right-after BIKE sessions of increasing duration to compare features of locomotor-like patterns.

Initially, we applied a 10-min session of BIKE to five samples, without observing any significant increase in the number of oscillations (96.62 ± 37.83 of pre-BIKE control; W = -4, P = 0,625, Wilcoxon signed rank test), cumulative depolarization peak (100.24 ± 5.39 % of pre-BIKE control; $t_{(4)}$ = -0.402, P = 0.709, paired t-test) or amplitude of FL oscillations (100.55 ± 2.87 % of pre-BIKE control; $t_{(4)}$ = -0.569, P = 0.600, paired t-test).

Thereafter, we considered prolonged BIKE sessions. In an exemplar experiment, episodes of FL were electrically-elicited by DR stimulation before and after 30 minutes of training (see DC-coupled traces in Fig. 6 A, B). In pre-BIKE control conditions, the electrical stimulation protocol induced a cumulative depolarization with 8 locomotor-like oscillations (Fig. 6 A). At the end of 30-min BIKE, the number of oscillations increased to 12 (Fig. 6 B). Pooled data from nine independent samples showed a statistically significant increase in the number of oscillations at the end of a 30-min BIKE session compared to pre-BIKE control (pre-BIKE control: 11 ± 4 FL cycles; after 30 minutes BIKE: 14 ± 4 FL cycles; W = 36, P = 0.008, Wilcoxon signed rank test). However, the number of oscillations diminished to initial values 20 min after ceasing BIKE training (Fig. 6 C, 11 ± 3 FL cycles; $\chi^2_{(2)}$ = 8.087, P = 0.012, Friedman repeated measures ANOVA on ranks, n = 6). Conversely, training did not affect the

amplitude of FL cycles (0.123 ± 0.088 mV in pre-BIKE control; 101.99 ± 25.82 % of pre-BIKE control after 30-mins BIKE and 123.18 ± 46.28 % of pre-BIKE control after 20 min post-BIKE rest; $H_{(2)} = 0.286$, P = 0.867, Kruskal-Wallis one-way ANOVA on ranks, n = 9, 9, 6) nor the peak of cumulative depolarization (0.538 ± 0.393 mV in pre-BIKE control; 111.89 ± 39.79 after 30-mins BIKE and 131.89 ± 43.31 % of pre-BIKE control after 20 min post-BIKE rest; $H_{(2)} = 0.364$, P = 0.833, Kruskal-Wallis one-way ANOVA on ranks, n = 9, 9, 6). Surprisingly, an extended training session of 90 minutes brought the number of FL cycles back to pre-BIKE control levels (W = -22, P = 0.148, Wilcoxon signed rank test, n = 8) and vanished the previous transitory FL facilitation induced by 30 min of BIKE (Fig. 6 D; 61.20 ± 23.38 % of 30 min BIKE; $U_{(8, 9)} = 8$, P = 0.008, Mann-Whitney rank sum test, n = 9, 8). Sham experiments reported that the *in vitro* maintenance for 90 min did not affect number of locomotor-like oscillations (W = -1, P = 1.000, Wilcoxon signed rank test, n = 3) nor cumulative depolarization (W = 2, P = 0.750, Wilcoxon signed rank test, n = 3).

A long session of BIKE depresses VR reflexes

To explore whether the lack of FL facilitation after 90 min BIKE was due to a depression in sensory-motor connections caused by long pedaling, we studied the sensory-motor reflex arc through the delivery of single pulses at low intensity (1xTh; 30.53 ± 9.66 μA) to a DR (T13 or L1), while recording potentials from the homologous VR. For a sample DC-coupled trace (Fig. 7 A), a long BIKE session stably reduced the area of DRVRPs for up to one hour after session end, but did not affect the peak of DRVRPs. Time course from many experiments (Fig. 7 B) demonstrated that the area of DRVRPs progressively decreased over longer BIKE durations, with a significant reduction at the end of session (90 min; $F_{(7, 91)} = 7.780$, $P \leq 0.001$, one-way repeated measures ANOVA followed by post-hoc analysis with Bonferroni t-test versus pre-BIKE control, n = 14). A subgroup of experiments, in which VR reflexes were not affected by a single 30-minute BIKE session (peak: $F_{(4, 16)} = 0.655$, P = 0.632, one-way repeated measures ANOVA, n = 5; area: $F_{(4, 16)} = 0.822$, P = 0.530, one-way repeated measures ANOVA, n = 5), confirmed that BIKE sessions shorter than 90 min did not affect the area of DRVRPs. Moreover, single pulses delivered during long sham experiments confirmed that long recordings did not significantly deteriorate the area of DRVRPs (Fig. 7 C; P = 0.971, one-way ANOVA, n = 8, 6, 5, 6).

A long session of BIKE increases spontaneous post-synaptic currents and membrane resistance of motoneurons

To identify whether the depressing effect of long BIKE applications corresponds to potential alterations in motoneuronal excitability, we performed whole-cell patch clamp recordings on single antidromically-identified motoneurons. These measurements were performed on a perpendicular upright arrangement of the isolated cord (Fig. 8 A) and lasted for up to five hours after termination of 90-min of BIKE or sham experiments.

Frequency of currents recorded in VC mode from single motoneurons increased after training, compared to sham experiments (Fig. 8 C, upper trace, and plot in D; $U_{(32, 33)} = 282.5$, $P = 0.001$, Mann-Whitney rank sum test, $n_{cells} = 32, 33$, $n = 11, 14$), indicating an augmentation of input converging onto the motoneuron. However, this input was not sufficient to generate a spontaneous firing in CC mode, despite the presence of a more ragged baseline (Fig. 8 C, bottom trace), in line with the reduced membrane resistance of motoneurons after training (Fig. 8 E, F; $t_{(15)} = 2.182$, $P = 0.04$, t-test, $n_{cells} = 5, 12$, $n = 5, 8$).

After selecting single events, we obtained average traces for fast-decaying sPSCs (Fig. 8 G; $\tau = 5.43 \pm 1.17$ ms, $n_{cells} = 79$, $n = 33$) and slow-decaying sPSCs (Fig. 8 H; $\tau = 20.10 \pm 6.61$ ms, $n_{cells} = 80$, $n = 33$), which indicate that BIKE increased frequency of both fast (Fig. 8 I; $U_{(32, 33)} = 361.5$, $P = 0.029$, Mann-Whitney rank sum test, $n_{cells} = 32, 33$, $n = 11, 14$) and slow currents (Fig. 8 J; $U_{(32, 33)} = 357.5$, $P = 0.026$, Mann-Whitney rank sum test, $n_{cells} = 32, 33$, $n = 11, 14$). Moreover, kinetic analysis of currents revealed no difference between motoneurons undergoing 90-minute training protocols vs. sham (data not shown).

Then, we selectively discriminated between fast glutamate-related currents and slow GABA/glycine-related currents through patch clamp recordings at reversal potentials for Cl^- and Na^+/K^+ cations. VC recordings from BIKE-trained and sham motoneurons at the two different holding potentials indicated that frequency of both fast ($U_{(5, 10)} = 9$, $P = 0.05$, Mann-Whitney rank sum test, $n_{cells} = 5, 10$, $n = 4, 6$) and slow currents ($U_{(5, 10)} = 9$, $P = 0.05$, Mann-Whitney rank sum test, $n_{cells} = 5, 10$, $n = 4, 6$) increased with BIKE.

We also analyzed the effects of 30-mins of BIKE over sPSCs recorded from motoneurons. Compared to sham experiments, input frequency to single motoneurons remained unchanged (sPSCs in sham preparations: 1.87 ± 2.32 Hz, $n_{cells} = 17$, $n = 6$; sPSCs in BIKE preparations: 1.54 ± 1.33 Hz, $n_{cells} = 20$, $n = 9$; $U_{(17, 20)} = 156$, $P = 0.681$, Mann-Whitney rank sum test), as did fast-decaying (fast sPSCs in sham preparations: 1.19 ± 2.06 Hz, $n_{cells} = 17$, $n = 6$; fast sPSCs in BIKE preparations: 0.60 ± 0.89 Hz, $n_{cells} = 20$, $n = 9$; $U_{(17, 20)} = 162.5$, $P = 0.831$, Mann-Whitney rank sum test) and slow-decaying sPSCs (slow sPSCs in sham preparations: 0.69 ± 0.73 Hz, $n_{cells} = 17$, $n = 6$; slow sPSCs in BIKE preparations: 0.94 ± 0.85, $n_{cells} = 20$, $n = 9$; $U_{(17, 20)} = 134.5$, $P = 0.286$, Mann-Whitney rank sum test). Likewise, membrane

resistance of single motoneurons was unaffected by 30-mins BIKE, as measured by comparing a random sample of five cells from four trained preparations to a group of nine cells from four sham experiments ($t_{(13)}$ = -0.771, P = 0.455, t-test).

Training modulates dorsal spinal networks

To clarify whether BIKE could actually affect synaptic transmission in the dorsal cord, we first recorded DRDRPs, both in pre-BIKE control conditions and after training. At the end of 30 minutes of BIKE, peaks of DRDRPs were unchanged (110.94 ± 26.18 % of pre-BIKE control) and remained similar to baseline values for up to 1 hour of post-BIKE rest (111.75 ± 27.46 % of pre-BIKE control; $\chi^2_{(4)}$ = 1.440, P = 0.837, Friedman repeated measures ANOVA on ranks, n = 5). When training was prolonged to 90 min, the peak of DRDRPs increased by 40% right after BIKE (Fig. 9 A) and the amplitude of responses remained higher than pre-BIKE control, even after a long post-BIKE rest (time course in Fig. 9 B; $\chi^2_{(6)}$ = 14.657, P = 0.023, Friedman repeated measures ANOVA on ranks followed by Dunn's test versus control, n = 5). However, to explore whether peaks of DRDRPs become higher after a long post-BIKE rest, a pairwise statistical analysis was performed only among the data points collected at post-BIKE rest in Fig. 9 B, showing no variation in DRDRPs at different time points during post-BIKE rest ($\chi^2_{(5)}$ = 9.914, P = 0.078, Friedman repeated measures ANOVA on ranks, n = 5). Moreover, spontaneous antidromic activity recorded from left L2 DR in DC mode during training displays an increased frequency of antidromic discharges (Fig. 9 C). Pooled data from many experiments point out that the power spectrum magnitude of spontaneous DR activity significantly increased upon BIKE start (Fig. 9 D) and values of DR antidromic discharges remained significantly higher than pre-BIKE control throughout training ($F_{(6, 18)}$ = 14.865, $P \leq 0.001$, one-way repeated measures ANOVA followed by post-hoc analysis with Bonferroni t-test versus control, n = 4).

Ninety minutes of passive mobilization long-lastingly increase spontaneous dorsal discharges

To explore whether spinal circuit excitability is affected by longer BIKE sessions and can persist even after the end of pedaling, spontaneous activity was continuously recorded in DC-mode from cut L2 spinal roots before, during and at the end of a 90-min session, as well as for over two hours of post-BIKE rest (Fig. 10).

During a 20-min pre-BIKE control period, VR bursts emerged (Fig. 10 A, left panels) while measuring a simultaneous intense tonic activity from DRs (Fig. 10 A, left panels). Recordings continued during the subsequent 90-min BIKE period (Fig. 10 A, middle panels) and showed

an increase in DR activity (in line with Fig. 9 C, D), while VR discharges remained unaffected (compare with Fig. 5). Twenty minutes after cessation of BIKE, only DR activity strongly augmented both in frequency and amplitude (Fig. 10 A, right panels). From the same experiment, FFTs described the rhythmic activity of all the VRs and the single DR during BIKE. No 0.5 Hz rhythmic component was detected, indicating the lack of any phase relationship between pedaling pace and spontaneous VR activity (Fig. 10 B, top and middle plots). On the contrary, antidromic DR activity was phase-related with pedaling, as confirmed by the peak of discharge frequency observed closely around 0.5 Hz (Fig. 10 B, bottom plot), which was absent from DR activity during pre-BIKE control and post-BIKE rest (not shown).

Power spectrum magnitude from many experiments confirmed that VR discharges were not significantly affected by 90 min training (Fig. 10 C; $t_{(7)} = 2.119$, $P = 0.072$, paired t-test, $n = 8$), although the amplitude of events recorded from DRs was significantly higher than pre-BIKE control (Fig 10 D; $t_{(7)} = -4.058$, $P = 0.005$, paired t-test, $n = 8$).

To identify the minimal protocol duration to elicit a significant increase in spontaneous dorsal activity after training, 30 min-long BIKE sessions were applied in sequence while DR rhythm magnitude was monitored at the end of each session (Fig. 10 E). Cumulative BIKE sessions lasting less than 90 minutes did not change magnitude of dorsal discharges, while longer sessions evoked a statistical variation in DR rhythmicity that persisted after turning off BIKE (Fig. 10 F; $F_{(3, 9)} = 5.010$, $P = 0.026$, one-way repeated measures ANOVA followed by post-hoc analysis with Bonferroni t-test versus control, $n = 4$).

In a subset of experiments, the activity recorded from DRs and VRs, expressed as RMS of the power spectrum, was calculated in slots of 20 min for up to 140 minutes of post-BIKE rest. VR spontaneous activity was not significantly affected by 90 min BIKE even in the long run (see time course in Fig. 10 G, in grey; $F_{(7, 28)} = 2.102$, $P = 0.077$, one-way repeated measures ANOVA, $n = 5$). Conversely, DR discharges remained significantly higher than pre-BIKE control for the entire observation period (Fig. 10 G, in black; $F_{(7, 28)} = 5.726$, $P < 0.001$, one-way repeated measures ANOVA followed by post-hoc analysis with Bonferroni t-test versus pre-BIKE control, $n = 5$).

Discussion

In this study, we associated intra- and extra-cellular electrophysiological recordings with an innovative robot that generates consistent afferent input to DRs. We proved that 30 minutes of alternating passive limb mobilization increases the number of locomotor-like oscillations induced by DR electrical stimulation, without affecting VR reflexes and DR potentials. This

facilitatory effect on the locomotor CPG was lost with longer training sessions, which also reduced the area of VR reflexes and increased both frequency of currents recorded from single motoneurons and antidromic discharges recorded from DRs.

A novel robotic instrument to induce a real alternate movement of hindlimbs in vitro

We invented a new robotic device, BIKE, for the standardized mobilization of limbs in an isolated neonatal rat spinal cord preparation with legs attached. Our innovative model proved suitable to trace an earlier modulation of spinal networks before, during and up to five hours after the end of passive exercise. In the past decades, the modulatory effects of actual limb movement on the *in vitro* CPG output have been studied using several experimental models (Wheatley and Stein, 1992; Hayes et al., 2009). In particular, Hayes and collaborators (2009) pharmacologically activated the CPG to induce real locomotion, and then studied how the resulting limb movements modulated the ongoing neurochemically-driven CPG rhythmic pattern. Our model, on the other hand, induces mere passive limb movement to study how a session of passive mobilization can facilitate locomotor patterns. Our preparation allows to study the role of afferent feedback evoked by dorsal spinal nerves during the sole limb movement, which cannot be explored if the whole preparation is in contact with neurochemicals. Indeed, neurochemicals would inevitably contaminate afferent volleys, inducing antidromic rhythmic activity along spinal dorsal networks (Kremer and Lev-Tov, 1998) and increasing excitability of spinal ganglia (Lovinger and Weight, 1988; Cardenas et al., 2001).

In this study, BIKE generated stereotyped rotations at the same average frequency as a neurochemically-induced (NMDA+5HT) FL previously evoked from the same preparation. Moreover, skin compression experiments demonstrated that afferent pathways still convey input from the periphery to the dorsal spinal cord, even though oxygenation of hindlimb tissues in our preparation was probably perturbed after dissection and for the entire experimental protocol due to the absence of blood circulation.

Future studies can exploit BIKE's ability to variate exercise frequency during each pedaling session to define the optimal intensity of training and assess how variations in pedaling speed affect spinal networks. Moreover, versatility of BIKE also allows to assess the importance of rhythmic, bilateral alternation vs. non-stereotyped movements to improve CPG functionality as a result of input variability (Ziegler et al., 2010). These perspectives would provide an important link to some current open questions about neurorehabilitation strategies in humans.

Suggested origin of afferent input induced by BIKE

Using *en passant* recordings from DRs during BIKE, we consistently observed afferent volleys of a yet unclear origin. Both the activity of the locomotor CPG and the adaptation of locomotion to the environment are facilitated by sensory stimulation and are mainly provided by the sensory feedback from both load bearing structures and mechanoreceptors of the hip (Dietz et al., 2002). In our model, cyclic pressure of the foot plant with each pedaling movement recruits only a limited number of load receptors, as limbs are in an antigravity upside-down position. Nevertheless, experiments with electrical skin stimulation indicate that our model can still exploit cutaneous afferents. Although, cutaneous responses can also facilitate locomotor activity in spinal and decerebrate preparations (Pearson and Rossignol, 1991; Hiebert and Pearson, 1999), input from cutaneous receptors physiologically modulates the activity of lumbar locomotor circuits mostly by recruiting supraspinal systems, which are absent in our preparation (Drew et al., 2004; McVea et al., 2007; Wong et al., 2018). As shown by afferent volleys recorded in this study following mechanical compression of the paw, input from nociceptive cutaneous afferents are present in our preparation and they might be recruited during BIKE to further modulate the CPG (Mandadi and Whelan, 2009). Pedaling evokes a hip joint range of motion that can generate a proprioceptive input, in turn facilitating locomotion. However, proprioceptors are poor stretch transducers without any alpha-gamma recruitment to shorten and/or increase intrafusal fiber stiffness, thus rendering their contribution only marginal in our model.

It should be noted that the paucity of afferent input reflects the low amplitude of discharges recorded in our study and might also be linked to immaturity of the preparation, which reaches full development of afferent pathways only in the first three postnatal weeks (Fitzgerald et al., 1994). Nevertheless, the same afferent feedback from the periphery to the central spinal circuits present at birth is only weakly inhibited pre-synaptically. Therefore, even a scarce peripheral feedback during early postnatal stages (Sonner and Ladle, 2013) might contribute to optimally modulate the ontogeny of spinal circuits (Vinay et al., 2002).

Overall, BIKE increased afferent activity with a distinctive frequency spectrum, where the rhythmic component of pedaling stands out from a highly variable background activity. Interestingly, the combination of a baseline noisy input and a phasic component at the frequency of stepping resembles the stimulating protocol that optimally activates the locomotor CPG in the neonatal rat isolated spinal cord (Dose and Taccola, 2016).

Mechanisms of BIKE in facilitating excitatory and inhibitory input, with different timing

BIKE generated both excitatory and inhibitory effects. A short application of BIKE transitorily increased the number of locomotor-like oscillations induced by trains of dorsal stimuli. On the other hand, a longer application abolished this effect and reduced the area of DRVRPs. At the same time, a longer application also potentiated antidromic discharges, whether spontaneous or induced by dorsal stimulation, lasting for even several hours after the end of training. The increased spontaneous DRPs and evoked DRDRPs parallel the decrease in DRVRPs, likely due to deletion of input incoming from DR stimulation, determined by spike occlusion at the level of sensory afferents. An additional explanation might reside in an increased concentration of GABA, generating a two-stage effect: pre-synaptically depolarizing primary afferents that originate antidromic DR discharges, and post-synaptically hyperpolarizing post-synaptic targets, in turn inhibiting motor reflexes.

The analysis of current kinetics, intracellularly recorded from motoneurons after 90-min BIKE, revealed an increased frequency of fast spontaneous currents, mainly attributed to AMPA receptors (Hestrin, 1993; Wyllie et al., 1994; Galante et al., 2000), paired with increased slow spontaneous currents, putatively ascribed to a GABAergic nature (Lewis and Faber, 1996; Galante et al., 2000). The increased number of input directed to motoneurons is consistent with an augmented release of vesicles from presynaptic terminals (Katz and Miledi, 1967). Conversely, peak amplitude of spontaneous PSCs remained unaltered, presumably indicating that the probability of channel opening in motoneurons was unaffected (Katz and Miledi, 1967). These results suggest that a prolonged training mainly affects pre-motoneuronal networks rather than motoneuron membranes. Unfortunately, the longer time frame needed to start patch clamp recordings did not allow us to investigate properties of spontaneous currents right after the shorter BIKE sessions that transiently facilitated locomotor networks. Therefore, we cannot exclude that some modifications in the biophysical properties of motoneurons did transitorily take place during FL facilitation induced by short BIKE sessions.

The most parsimonious explanation of the effects observed in this study is that excitatory and inhibitory contributions were recruited with a different timing during BIKE. This hypothesis, although not tested in this study, would predict an increase in DRVRPs over short BIKE periods. However, FL facilitation seen for shorter training sessions might reflect an early increase in spinal excitation, in line with the facilitation of weak electrical stimulation in the presence of low concentrations of glutamatergic agents (Dose and Taccola, 2012). Moreover, this study indicates that BIKE increases fast spontaneous PSCs attributed to AMPA glutamatergic receptors.

Nevertheless, AMPA input on the motoneuron might be overwhelmed by longer sessions of BIKE because of the appearance, or the progressive increase, of GABAergic post-synaptic input (Fontana et al., 2001), which have been reported to depress FL (Cazalets et al., 1994; Cowley and Schmidt, 1995). However, we could not test the selective pharmacological antagonism of AMPA or GABA receptors, as these drugs would have interfered with the expression of FL (Bracci et al., 1996b; Beato et al., 1997).

An alternative explanation suggests that potentiation of AMPA receptors (and the corresponding facilitation of FL) is lost with a prolonged BIKE application because of the desensitization of AMPA channels (Ballerini et al., 1995; Tsvyetlynska et al., 2005). Nonetheless, this hypothesis seems unlikely, since fast currents on the motoneuron are augmented after 90-min BIKE. Moreover, in correspondence to longer BIKE sessions, motoneuron membrane resistance was found to diminish, in line with previous reports on trained adult rats (Beaumont et al., 2004).

Apart from changes in motoneurons, efficacy of BIKE relies on a more complex mechanism, potentially affecting many other properties of the spinal cord. As a matter of fact, the state of CPG interneurons is perturbed by afferent input (Burke, 1999), primary afferent depolarization and other sensorimotor functions (Ménard et al., 2002; Hayes et al., 2012). Overall, BIKE enhances spontaneous synaptic transmission within the spinal network, in line with training affecting the proportion of inhibitory vs. excitatory boutons in rat motoneurons (Ichiyama et al., 2011).

Clinical perspectives

We are aware that neonatal rodents are not the best suited model to understand the mechanisms of passive pedaling in humans, adults in particular. Indeed, P0–P4 neonatal rats cannot bear their own weight and descending and sensory input to motoneurons, as well as their membrane properties, are still at an immature developing stage (Vinay et al., 2002; Clarac et al., 2004). Nevertheless, these models share important basic characteristics with adult animals and humans. In the present study, the transient facilitation of locomotor patterns with a precise timing after passive cycling might suggest the existence of an optimal therapeutic window for co-administering pharmacological agents and neurorehabilitation to activate spinal locomotor circuits after SCI (NCT01621113, NCT01484184, ClinicalTrials.gov).

Acknowledgments: We are grateful to Prof. Andrea Nistri for data discussion, John Fischetti for technical support in building BIKE and Dr. Elisa Ius for her excellent assistance in preparing the manuscript. We thank Dr. Vladimir Rancic and Dr. Alessandra Fabbro for help with patch clamp recordings and analysis. We are also grateful to Rosmary Blanco for her assistance with peripheral nerve experiments.

Declarations of interest: none.

Funding: This research did not receive any specific grant from funding agencies in the public, commercial, or not-for-profit sectors.

References

Acevedo JM, Díaz-Ríos M (2013) Removing sensory input disrupts spinal locomotor activity in the early postnatal period. J Comp Physiol A Neuroethol Sens Neural Behav Physiol 199:1105–1116.

Ballerini L, Bracci E, Nistri A (1995) Desensitization of AMPA receptors limits the amplitude of EPSPs and the excitability of motoneurons of the rat isolated spinal cord. Eur J Neurosci 7:1229–1234.

Barry PH (1994) JPCalc, a software package for calculating liquid junction potential corrections in patch-clamp, intracellular, epithelial and bilayer measurements and for correcting junction potential measurements. J Neurosci Methods 51:107–116.

Beato M, Bracci E, Nistri A (1997) Contribution of NMDA and non-NMDA glutamate receptors to locomotor pattern generation in the neonatal rat spinal cord. Proc Biol Sci 264:877–884.

Beaumont E, Houlé JD, Peterson CA, Gardiner PF (2004) Passive exercise and fetal spinal cord transplant both help to restore motoneuronal properties after spinal cord transection in rats. Muscle Nerve 29:234–242.

Bouhadfane M, Tazerart S, Mogrich A, Vinay L, Brochard F (2013) Sodium-mediated plateu potentials in lumbar motoneurons of neonatal rats. J Neurosci 33:15626–15641.

Bracci E, Ballerini L, Nistri A (1996a) Localization of rhythmogenic networks responsible for spontaneous bursts induced by strychnine and bicuculline in the rat isolated spinal cord. J Neurosci 16:7063–7076.

Bracci E, Ballerini L, Nistri A (1996b) Spontaneous rhythmic bursts induced by pharmacological block of inhibition in lumbar motoneurons of the neonatal rat spinal cord. J Neurophysiol 75:640–647.

729 Brumley MR, Guertin PA, Taccola G (2017) Multilevel analysis of locomotion in immature
730 preparations suggests innovative strategies to reactivate stepping after spinal cord injury. Curr
731 Pharm Des 23:1764–1777.
732
733 Burke RE (1999) The use of state-dependent modulation of spinal reflexes as a tool to
734 investigate the organization of spinal interneurons. Exp Brain Res 128:263–277.
735
736 Cardenas LM, Cardenas CG, Scroggs RS (2001) 5HT increases excitability of nociceptor-like
737 rat dorsal root ganglion neurons via cAMP-coupled TTX-resistant Na(+) channels. J
738 Neurophysiol 86:241–248.
739
740 Cazalets JR, Sqalli-Houssaini Y, Clarac F (1994) GABAergic inactivation of the central
741 pattern generators for locomotion in isolated neonatal rat spinal cord. J Physiol 474:173–181.
742
743 Chopek JW, MacDonell CW, Gardiner K, Gardiner PF (2014) Daily passive cycling
744 attenuates the hyperexcitability and restores the responsiveness of the extensor monosynaptic
745 reflex to quipazine in the chronic spinally transected rat. J Neurotrauma 31:1083–1087.
746
747 Chopek JW, Sheppard PC, Gardiner K, Gardiner PF (2015) Serotonin receptor and KCC2
748 gene expression in lumbar flexor and extensor motoneurons posttransection with and without
749 passive cycling. J Neurophysiol 113:1369–1376.
750
751 Cifra A, Mazzone GL, Nani F, Nistri A, Mladinic M (2012) Postnatal developmental profile
752 of neurons and glia in motor nuclei of the brainstem and spinal cord, and its comparison with
753 organotypic slice cultures. Dev Neurobiol 72:1140–1160.
754
755 Clarac F, Brocard F, Vinay L (2004) The maturation of locomotor networks. Prog Brain Res
756 143:57-66.
757
758 Côté MP, Gandhi S, Zambrotta M, Houlé JD (2014) Exercise modulates chloride homeostasis
759 after spinal cord injury. J Neurosci 34:8976–8987.
760

761 Cowley KC, Schmidt BJ (1995) Effects of inhibitory amino acid antagonists on reciprocal
762 inhibitory interactions during rhythmic motor activity in the in vitro neonatal rat spinal cord. J
763 Neurophysiol 74:1109–1117.
764
765 Cowley KC, Schmidt BJ (1997) Regional distribution of the locomotor pattern-generating
766 network in the neonatal rat spinal cord. J Neurophysiol 77:247–259.
767
768 Deumens R, Mazzone GL, Taccola G (2013) Early spread of hyperexcitability to caudal
769 dorsal horn networks after a chemically-induced lesion of the rat spinal cord in vitro.
770 Neuroscience 229:155–163.
771
772 Dietz V, Müller R, Colombo G (2002) Locomotor activity in spinal man: significance of
773 afferent input from joint and load receptors. Brain 125:2626–2634.
774
775 Dietz V, Fouad K (2014) Restoration of sensorimotor functions after spinal cord injury. Brain
776 137:654–667.
777
778 Dingu N, Deumens R, Taccola G (2016) Electrical stimulation able to trigger locomotor
779 spinal circuits also induces dorsal horn activity. Neuromodulation 19:38–46.
780
781 Dose F, Taccola G (2012) Coapplication of noisy patterned electrical stimuli and NMDA plus
782 serotonin facilitates fictive locomotion in the rat spinal cord. J Neurophysiol 108:2977–2990.
783
784 Dose F, Taccola G (2016) Two distinct stimulus frequencies delivered simultaneously at low
785 intensity generate robust locomotor patterns. Neuromodulation 19:563-575.
786
787 Dose F, Deumens R, Forget P, Taccola G (2016) Staggered multi-site low-frequency
788 electrostimulation effectively induces locomotor patterns in the isolated rat spinal cord. Spinal
789 Cord 54:93–101.
790
791 Drew T, Prentice S, Schepens B, (2004) Cortical and brainstem control of locomotion. Prog.
792 Brain Res 143:251–261.
793

Dugan EA, Sagen J (2015) An intensive locomotor training paradigm improves neuropathic pain following spinal cord compression injury in rats. J Neurotrauma 32:622–632.

Fabbro A, Villari A, Laishram J, Scaini D, Toma FM, Turco A, et al (2012) Spinal cord explants use carbon nanotube interfaces to enhance neurite outgrowth and to fortify synaptic inputs. ACS Nano 6:2041–2055.

Fitzgerald M, Butcher T, Shortland P (1994) Developmental changes in the laminar termination of A fibre cutaneous sensory afferents in the rat spinal cord dorsal horn. J Comp Neurol 348:225–233.

Fontana G, Taccola G, Galante J, Salis S, Raiteri M (2001) AMPA-evoked acetylcholine release from cultured spinal cord motoneurons and its inhibition by GABA and glycine. Neuroscience 106:183–191.

Fulton BP, Walton K (1986) Electrophysiological properties of neonatal rat motoneurones studied in vitro. J Physiol 370:651–678.

Galante M, Nistri A, Ballerini L (2000) Opposite changes in synaptic activity of organotypic rat spinal cord cultures after chronic block of AMPA/kainate or glycine and GABAA receptors. J Physiol 523:639–651.

Getting PA (1989) Emerging principles governing the operation of neural networks. Annu Rev Neurosci 12:185–204.

Harkema SJ, Hillyer J, Schmidt-Read M, Ardolino E, Sisto SA, Behrman AL (2012) Locomotor training: as a treatment of spinal cord injury and in the progression of neurologic rehabilitation. Arch Phys Med Rehabil 93:1588–1597.

Hayes HB, Chang YH, Hochman S (2009) An in vitro spinal cord-hindlimb preparation for studying behaviorally relevant rat locomotor function. J Neurophysiol 101:1114–1122.

826 Hayes HB, Chang YH, Hochman S (2012) Stance-phase force on the opposite limb dictates
827 swing-phase afferent presynaptic inhibition during locomotion. J Neurophysiol 107:3168–
828 3180.
829
830 Hestrin S (1993) Different glutamate receptor channels mediate fast excitatory synaptic
831 currents in inhibitory and excitatory cortical neurons. Neuron 11:1083–1091.
832
833 Hiebert GW, Pearson KG (1999) Contribution of sensory feedback to the generation of
834 extensor activity during walking in the decerebrate Cat. J Neurophysiol 81:758-770.
835
836 Hubli M, Dietz V (2013) The physiological basis of neurorehabilitation--locomotor training
837 after spinal cord injury. J Neuroeng Rehabil 10:5.
838
839 Ichiyama RM, Broman J, Roy RR, Zhong H, Edgerton VR, Havton LA (2011) Locomotor
840 training maintains normal inhibitory influence on both alpha- and gamma-motoneurons after
841 neonatal spinal cord transection. J Neurosci 31:26–33.
842
843 Joseph MS, Tillakaratne NJ, de Leon RD (2012) Treadmill training stimulates brain-derived
844 neurotrophic factor mRNA expression in motor neurons of the lumbar spinal cord in spinally
845 transected rats. Neuroscience 224:135–144.
846
847 Juvin L, Simmers J, Morin D (2007) Locomotor rhythmogenesis in the isolated rat spinal
848 cord: a phase- coupled set of symmetrical flexion extension oscillators. J Physiol 583:115–
849 128.
850
851 Katz B, Miledi M (1967) A study of synaptic transmission in the absence of nerve impulses. J
852 Physiol 192:407–436.
853
854 Keeler BE, Liu G, Siegfried RN, Zhukareva V, Murray M, Houlé JD (2012) Acute and
855 prolonged hindlimb exercise elicits different gene expression in motoneurons than sensory
856 neurons after spinal cord injury. Brain Res 1438:8–21.
857
858 Kerkut GA, Bagust J (1995) The isolated mammalian spinal cord. Prog Neurobiol 46:1–48.
859

Kiehn O, Kjaerulff O (1996) Spatiotemporal characteristics of 5-HT and dopamine-induced rhythmic hindlimb activity in the in vitro neonatal rat. J Neurophysiol 75:1472–1482.

Kiehn O (2006) Locomotor circuits in the mammalian spinal cord. Annu Rev Neurosci 29:279–306.

Kjaerulff O, Barajon I, Kiehn O (1994) Sulphorhodamine-labelled cells in the neonatal rat spinal cord following chemically induced locomotor activity in vitro. J Physiol 478:265–273.

Klein DA, Tresch MC (2010) Specificity of intramuscular activation during rhythms produced by spinal patterning systems in the in vitro neonatal rat with hindlimb attached preparation. J Neurophysiol 104:2158–2168.

Kremer E, Lev-Tov A (1997) Localization of the spinal network associated with generation of hindlimb locomotion in the neonatal rat and organization of its transverse coupling system. J Neurophysiol 77:1155–1170.

Kremer E, Lev-Tov A (1998) GABA-receptor-independent dorsal root afferents depolarization in the neonatal rat spinal cord. J Neurophysiol 79:2581–2592.

Lewis CA, Faber DS (1996) Properties of spontaneous inhibitory synaptic currents in cultured rat spinal cord and medullary neurons. J Neurophysiol 76:448–460.

Loeb GE, Bak MJ, Duysens J (1977) Long-term unit recording from somatosensory neurons in the spinal ganglia of the freely walking cat. Science 197:1192–1194.

Lovinger DM, Weight FF (1988) Glutamate induces a depolarization of adult rat dorsal root ganglion neurons that is mediated predominantly by NMDA receptors. Neurosci Lett 94:314–320.

Mandadi S, Whelan PJ (2009) A new method to study sensory modulation of locomotor networks by activation of thermosensitive cutaneous afferents using a hindlimb attached spinal cord preparation. J Neurosci Methods 182:255–259.

Mandadi S, Hong P, Tran MA, Bráz JM, Colarusso P, Basbaum AI, Whelan PJ (2013) Identification of multisegmental nociceptive afferents that modulate locomotor circuits in the neonatal mouse spinal cord. J Comp Neurol 521:2870–2887.

Marchetti C, Beato M, Nistri A (2001) Alternating rhythmic activity induced by dorsal root stimulation in the neonatal rat spinal cord in vitro. J Physiol 530:105–112.

McVea DA, Pearson KG (2007) Long-lasting, context-dependent modification of stepping in the cat after repeated stumbling-corrective responses. J Neurophysiol 97:659–669.

Ménard A, Leblond H, Gossard JP (2002) Sensory integration in presynaptic inhibitory pathways during fictive locomotion in the cat. J Neurophysiol 88:163-171.

Molander C, Xu Q, Grant G (1984) The cytoarchitectonic organization of the spinal cord in the rat. I. The lower thoracic and lumbosacral cord. J Comp Neurol 230:133–141.

Nishimaru H, Kudo N (2000) Formation of the central pattern generator for locomotion in the rat and mouse. Brain Res Bull 53:661–669.

Nistri A, Taccola G, Mladinic M, Margaryan G, Kuzhandaivel A. (2010) Deconstructing locomotor networks with experimental injury to define their membership. Ann N Y Acad Sci 1198:242-251.

Pearson KG, Rossignol S (1991) Fictive motor patterns in chronic spinal cats. J Neurophysiol 66:1874-1887.

Sirois J, Frigon A, Gossard JP (2013) Independent control of presynaptic inhibition by reticulospinal and sensory inputs at rest and during rhythmic activities in the cat. J Neurosci 33:8055–8067.

Sonner PM, Ladle DR (2013) Early postnatal development of GABAergic of Ia proprioceptive afferent connections in mouse spinal cord. J Neurophysiol 109:2118–2128.

Stein RB (1995) Presynaptic inhibition in humans. Prog Neurobiol 47:533–544.

928
929 Taccola G (2011) The locomotor central pattern generator of the rat spinal cord in vitro is
930 optimally activated by noisy dorsal root waveforms. J Neurophysiol 106:872–884.
931
932 Taccola G, Olivieri D, D'Angelo G, Blackburn P, Secchia L, Ballanyi K (2012) A_1 adenosine
933 receptor modulation of chemically and electrically evoked lumbar locomotor network activity
934 in isolated newborn rat spinal cords. Neuroscience 222:191–204.
935
936 Tartas M, Morin F, Barrière G, Goillandeau M, Lacaille JC, Cazalets JR, Bertand SS (2010)
937 Noradrenergic modulation of intrinsic and synaptic properties of lumbar motoneurons in the
938 neonatal rat spinal cord. Front Neural Circuits 4:4.
939
940 Tsvyetlynska NA, Hill RH, Grillner S (2005) Role of AMPA receptor desensitization and the
941 side effects of a DMSO vehicle on reticulospinal EPSPs and locomotor activity. J
942 Neurophysiol 94:3951–3960.
943
944 Vinay L, Brocard F, Fellippa-Marques S, Clarac F (1999) Antidromic discharges of dorsal
945 root afferents in the neonatal rat. J Physiol Paris 93:359–367.
946
947 Vinay L, Brocard F, Clarac F, Norreel JC, Pearlstein E, Pflieger JF (2002) Development of
948 posture and locomotion: an interplay of endogenously generated activities and neurotrophic
949 actions by descending pathways. Brain Res Brain Res Rev 40:118–129.
950
951 Wheatley M, Stein RB (1992) An in vitro preparation of the mudpuppy for simultaneous
952 intracellular and electromyographic recording during locomotion. J Neurosci Methods
953 42:129–137.
954
955 Wyllie DJ, Manabe T, Nicoll RA (1994) A rise in postsynaptic Ca^{2+} potentiates miniature
956 excitatory postsynaptic currents and AMPA responses in hippocampal neurons. Neuron
957 12:127–138.
958
959 Wong C, Wong G, Pearson KG, Lomber SG (2018) Memory-guided stumbling correction in
960 the hindlimb of quadrupeds relies on parietal area 5. Cereb Cortex 28:561–573.
961

962 Ziegler MD, Zhong H, Roy RR, Edgerton VR (2010) Why variability facilitates spinal
963 learning. J Neurosci 30:10720–10726.
964

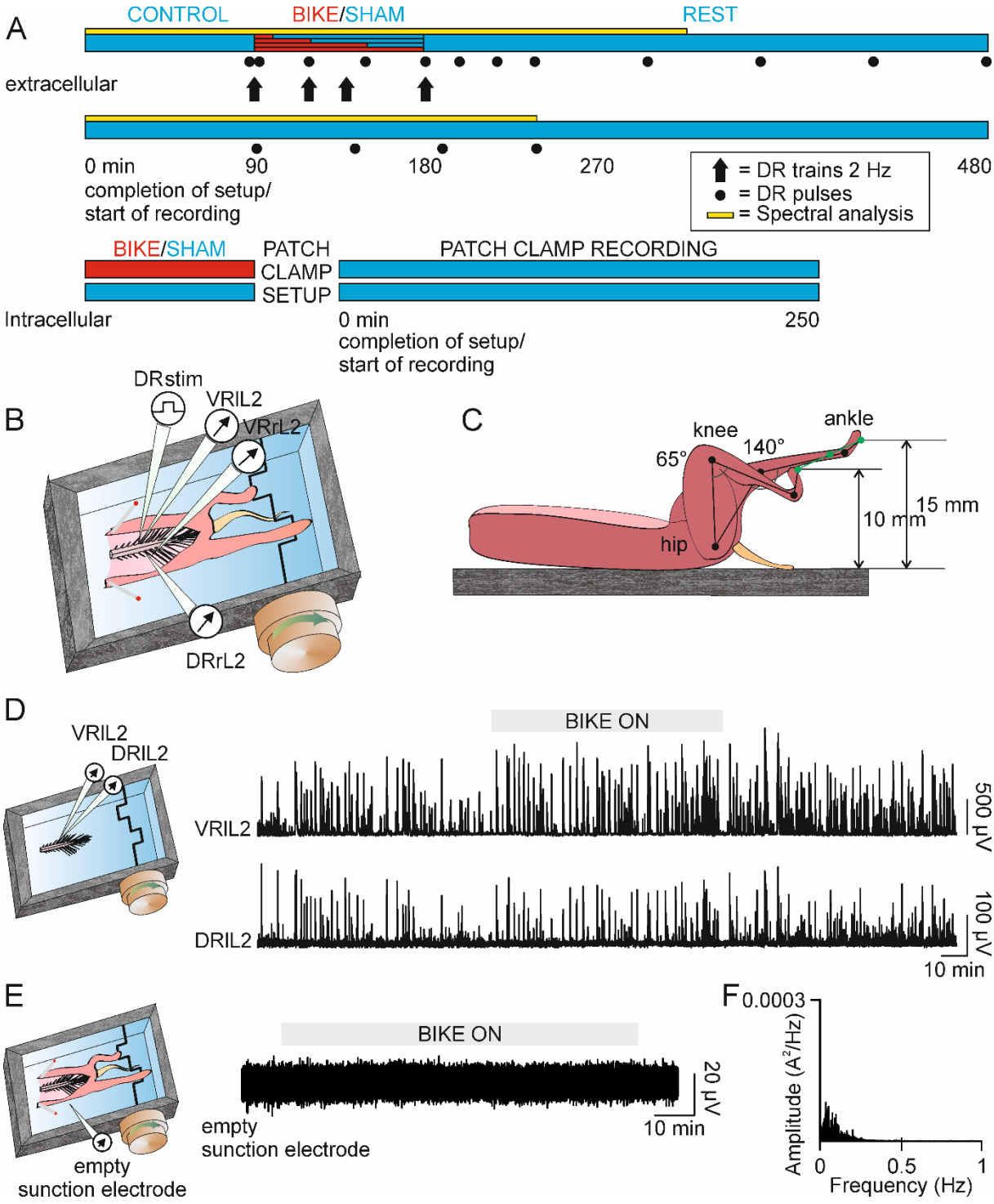

Figure 1. BIKE allows passive hindlimb movement while simultaneously recording from spinal roots.

A: Bars summarize protocols for extracellular (top bars) and patch clamp (bottom bars) experiments. Time zero was arbitrarily assigned to the beginning of each recording. The extracellular protocol consisted in a pre-BIKE control, a session of passive pedaling driven by BIKE (10, 30, 60 or 90 minutes; in red), and a long post-BIKE rest. Throughout the

experiment, spontaneous activity (yellow bar), evoked activity (black dots) and electrically-induced locomotor-like activity (black arrows) were continuously monitored. Sham experiments were also carried out and recordings were performed at comparable time points as BIKE preparations. As for patch clamp experiments, leg-attached preparations were first trained with BIKE (30- or 90-minute sessions) or maintained still in the BIKE recording chamber for an equivalent time interval. Then, each spinal cord was isolated and arranged for patch clamp recordings from lumbar motoneurons. **B**: The cartoon shows the experimental setup using a spinal cord with hindlimbs attached. Spinal roots were bilaterally dissected from the high thoracic region down to the second lumbar segment (L2) included. Preparation was maintained in a continuously superfused chamber, with hindpaws firmly fixed to the pedals of BIKE above the chamber. Speed rotation was adjusted through a stabilized power supply at around 30 cycles/min (0.5 Hz). Only forward movement was applied, as indicated by the arrow. Simultaneous recordings were performed with suction glass electrodes from both right (r) and left (l) L2 ventral roots (VRs) and from a single dorsal root (DR), either in the presence or in the absence of DR stimulation. **C**: A lateral view of the leg-attached isolated spinal cord on the BIKE device. The cartoon was modeled from goniometric measurements of knee joints taken from P2 animals. Actual angles might slightly change with younger or older subjects (P0, P4). **D**: Sample traces from VRlL2 and DRlL2 in an isolated spinal cord during BIKE pedaling show that BIKE does not induce any electrical interference to perturb electrophysiological recordings of spontaneous baseline activity. **E**: Background noise recorded with a glass electrode placed close to the L5 spinal segment demonstrates that passive hindlimb movement does not induce any baseline interference. **F**: The FFT analysis reports spectral analysis for the trace in **D**. Note the absence of any rhythmic components around the frequency of pedaling (0.5 Hz).

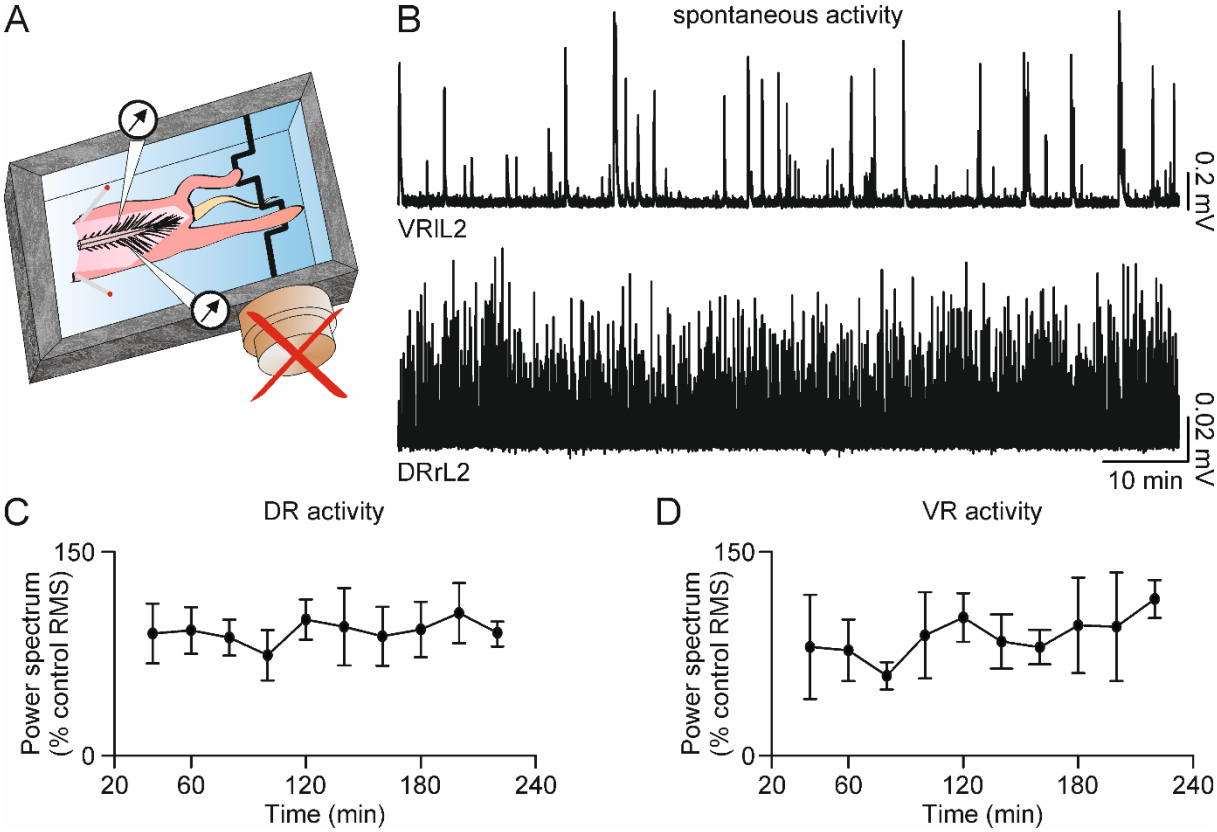

Figure 2. Spontaneous activity from spinal roots of the leg-attached isolated spinal cord is consistent over a long *in vitro* maintenance.

A: In sham experiments, preparations were set in the recording chamber following all usual procedures, apart from switching on BIKE, as depicted by the red cross on the rotor. **B**: Sample traces represent long recordings of spontaneous activity from VRlL2 (on the top) and DRrL2 (on the bottom). **C, D**: Time courses show the magnitude of the power spectrum calculated by 20-min bins of activity for DR discharges (**C**) and VR activity (**D**).

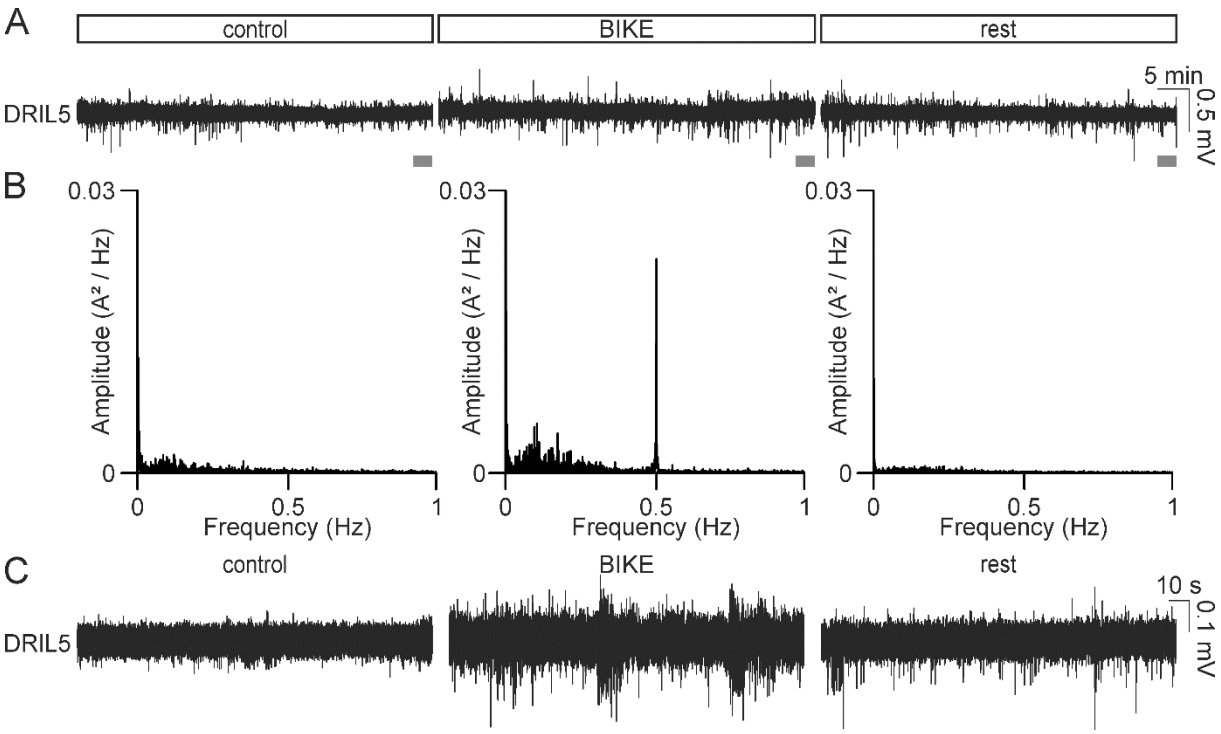

Figure 3. BIKE-induced passive training evokes afferent sensory feedback coupled with pedaling.

A: Sample traces were recorded during a 90-min pre-BIKE control (control), BIKE and post-BIKE rest (rest), as depicted by the protocol bars on top. Activity was derived from DRlL5 by applying a negative pressure on its surface through a suction glass electrode (*en passant* recordings). **B**: The FFT analysis for traces in **A** isolates a main frequency component at 0.5 Hz during BIKE (middle), which reflects the pedaling frequency. No components at 0.5 Hz could be detected either in pre-BIKE control (left) or at post-BIKE rest (right). **C**: Higher magnifications of traces in **A**, corresponding to grey rectangles, indicate the increase in afferent discharges during BIKE (middle) compared to pre-BIKE control (left) and post-BIKE rest (right).

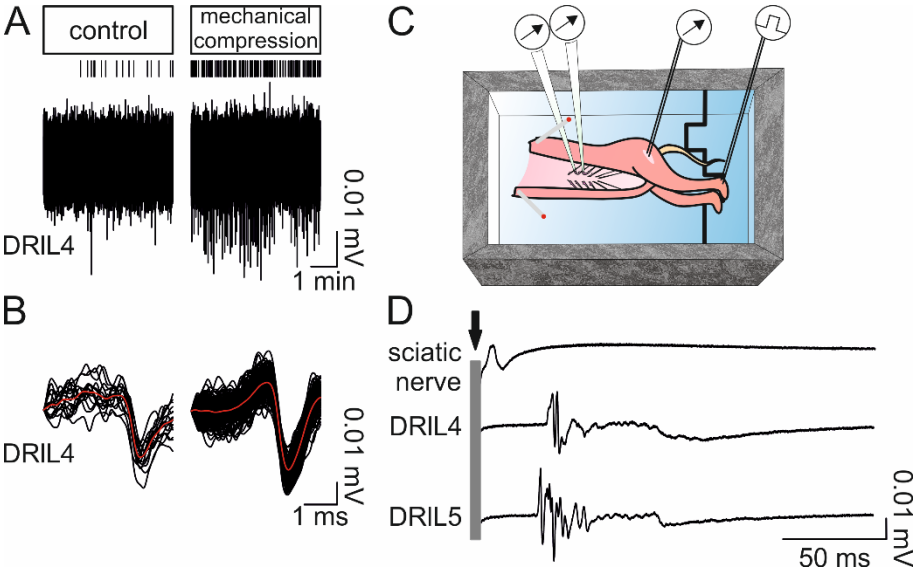

Figure 4. Afferent pathways to the spinal cord are recruited in our *in vitro* model.

A: Incoming discharges were recorded from a leg-attached preparation where the spinal cord was removed to allow recordings from the distal stump of DRlL4. Recordings were performed before and during a mechanical compression of the left hindpaw, as shown on top. Raster plots above traces highlight a greater incoming activity during peripheral mechanical compression of the left hindpaw. **B**: Identified events were superimposed and shown in black, while averaged traces were depicted in red. **C**: In a random group of experiments, leg-attached preparations deprived of the spinal cord were arranged in the BIKE recording chamber without any pedaling, as depicted by the cartoon. The left hindpaw was firmly fixed to the right pedal for single-pulse stimulation of the sural-innervated territory and for recording from the branch of the exposed sciatic nerve. Pairs of hooked needle electrodes were used for bipolar stimulation and recordings from the sciatic nerve. Moreover, monopolar recordings with suction glass electrodes were performed from the spinal stumps of DRlL4 and DRlL5. **D**: Average traces of 500 sweeps are reported. Compound action potentials could be elicited from both the sciatic nerve and, with a higher latency, from spinal afferent nerves L4 and L5. The grey rectangle on the left represents a 5-millisecond rectangular pulse applied to the sural territory on the left hindpaw.

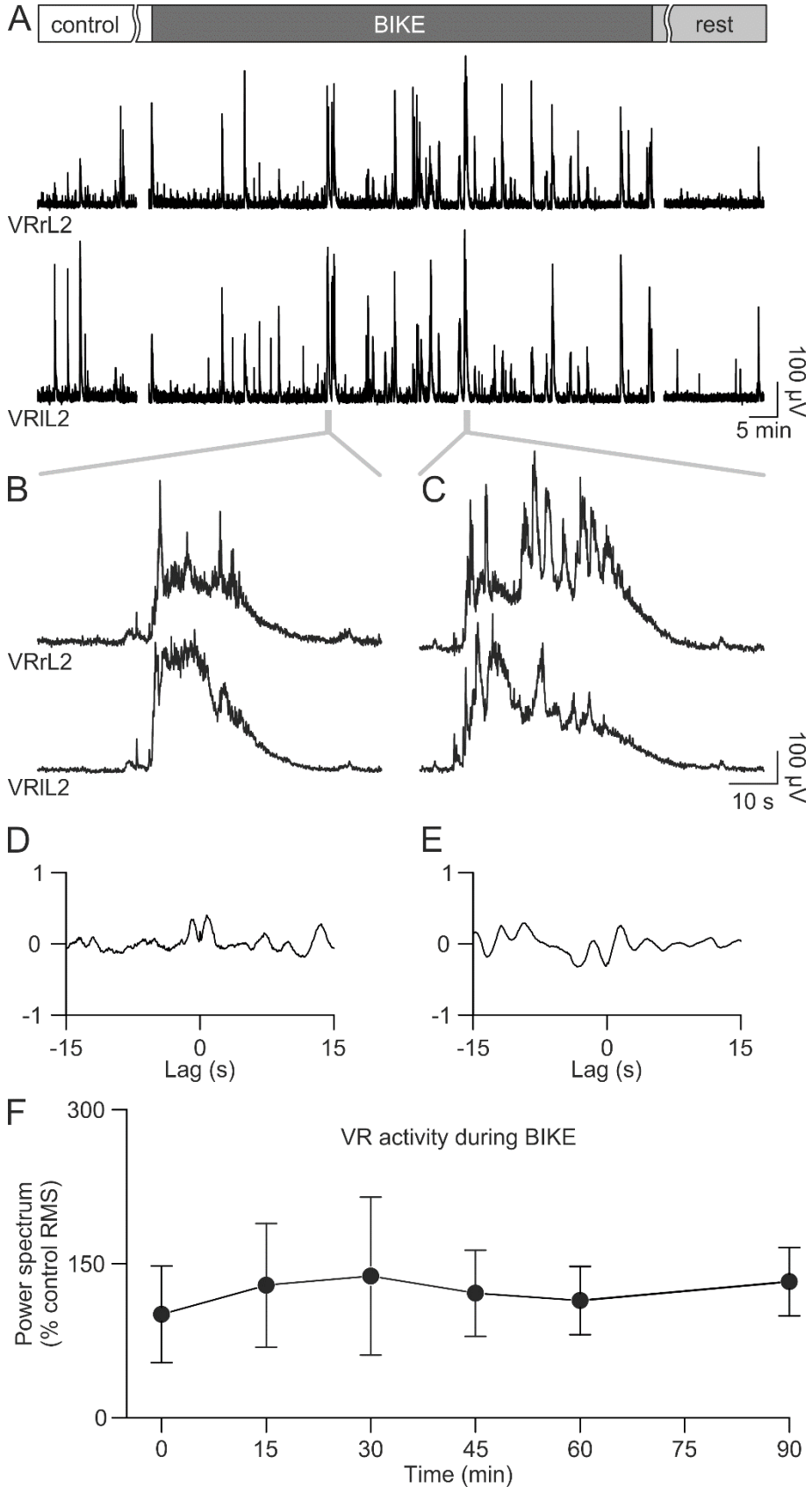

Figure 5. Long application of BIKE does not vary spontaneous VR activity.

A: Spontaneous activity was recorded from bilateral VRs L2 in pre-BIKE control (left), during a BIKE session (90 min; middle) and at the end of training (right). Traces are interrupted in correspondence to the artifacts from single or repetitive pulse stimulation (20 min). **B, C**: Magnifications of two bilateral bursts from VRs corresponding to the grey rectangles in **A**. **D, E**: Cross-correlograms between homosegmental L2s report poor phase coupling between a pair of VRs. **F**: The time course points out that magnitude of the power spectrum for VR spontaneous activity during BIKE was not significantly different from pre-BIKE control values.

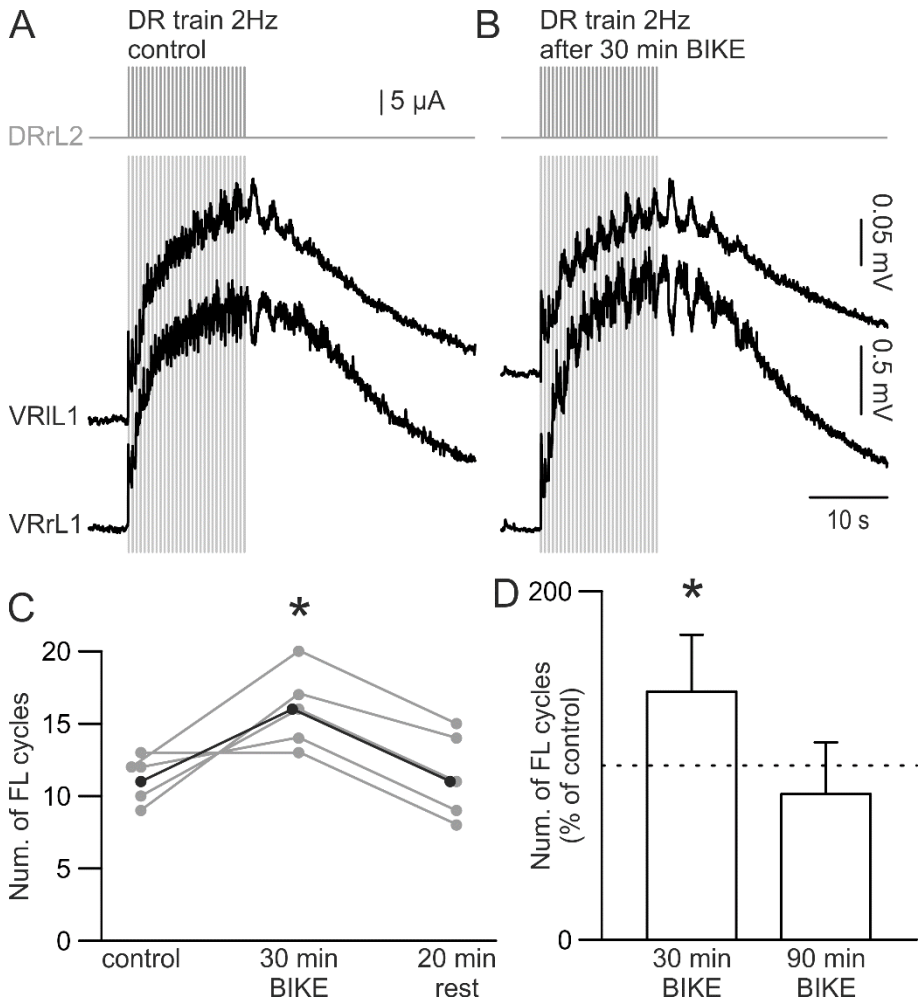

Figure 6. A 30-minute BIKE session transiently facilitates electrically-evoked FL.

A: Before BIKE, a train of stereotyped electrical stimuli (30 rectangular pulses; pulse duration = 0.1 ms; intensity = 45 µA, 3 x Th; frequency = 2 Hz) was delivered to DRrL2 (upper panel), inducing a characteristic episode of FL consisting in a cumulative depolarization with 8 superimposed alternating cycles recorded from homosegmental L1 VRs. **B**: At the end of a 30-minute BIKE session, the same train of pulses induced a higher number of locomotor-like oscillations. **C**: Plot summarizes, for six experiments, the time course related to the number of FL cycles induced by a train of stimuli, before BIKE, right after switching off BIKE (at the end of a 30-minute session) and after 20 minutes of post-BIKE rest. BIKE transiently augmented the number of FL cycles, which returned to pre-BIKE control values 20 minutes after the end of training (*; P = 0.012). Note that grey dots represent raw data and black dots indicate mean values. **D**: Histogram compares the average increase in the number of FL cycles induced by DR trains in preparations subjected to 30 or 90 min BIKE. The facilitatory

effect mediated by 30 minutes BIKE was lost if training was prolonged to 90 minutes (*; P = 0.008).

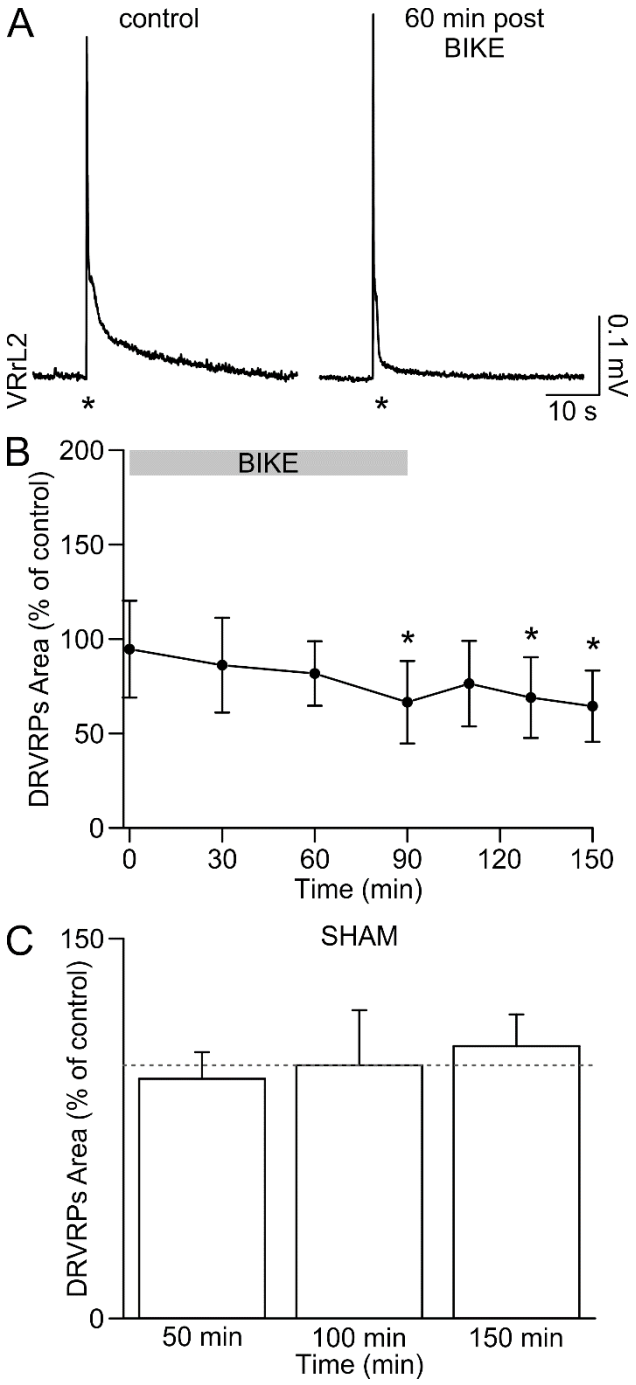

Figure 7. Only longer sessions of BIKE reduce the area of DRVRPs.

A: A spinal reflex (averaged traces from 10 sweeps) is induced by a single pulse (22 µA, Th, 100 µs) delivered to DRlT13 at the time indicated by the stars. In pre-BIKE control conditions (left), responses present an early peak followed by a slow decaying repolarization. One hour after a BIKE training session of 90 mins (right), the same pulse elicited a response of smaller area, while the peak remained unaffected. **B**: The time course plot summarizes mean values

collected from 14 experiments, showing a progressive reduction in the DRVRP area by prolonging the duration of the BIKE session. After 90 min BIKE, a significant reduction of the reflex response is reached and maintained for at least the following hour (*; P = <0.001). **C**: Bars report the area of DRVRPs in sham experiments (without any actual pedaling), at different time intervals. DRVRPs were monitored up to 150 min and they remained unchanged.

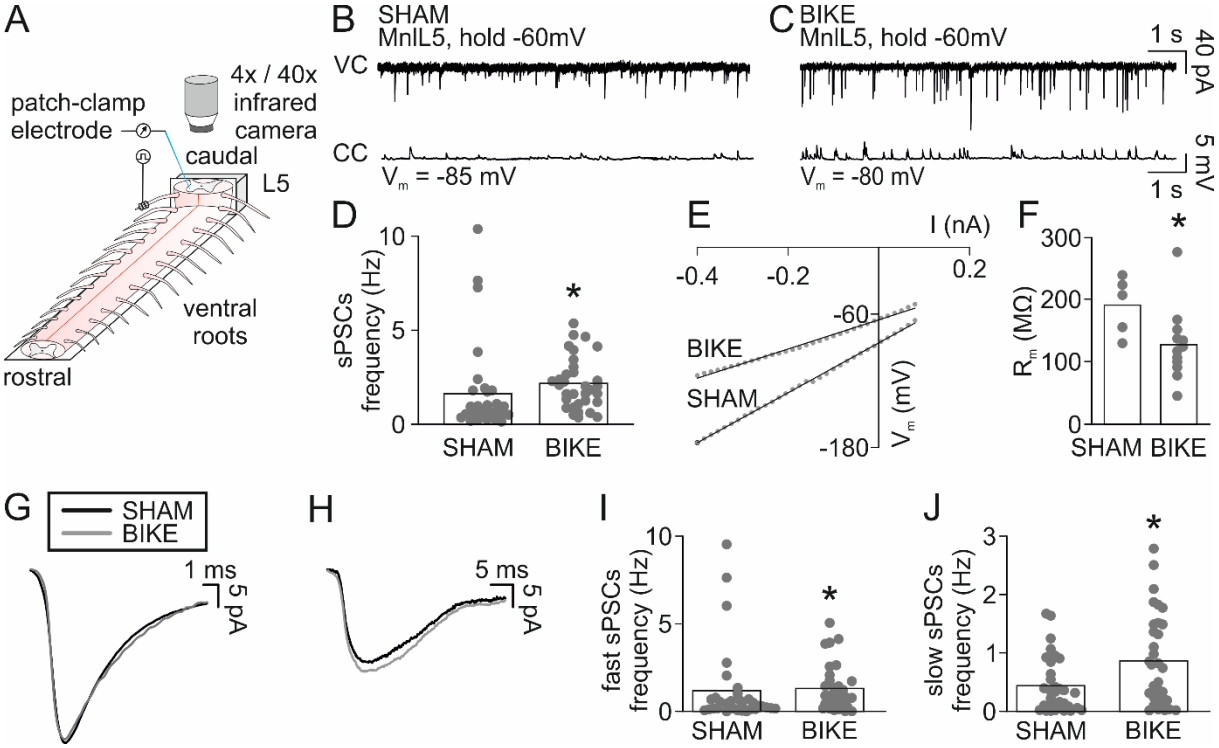

Figure 8. 90-minutes of BIKE affect synaptic transmission and membrane resistance of lumbar motoneurons.

A: Cords were isolated from leg-attached preparations at the end of BIKE training or sham experiments. The dorsal surface was glued on a plastic strip and bent in an upright position against a sylgard cube. In this configuration, L5 spinal segment faces upwards and motoneurons are visualized with an infrared camera for patch clamp recordings. L5 VR is antidromically stimulated using bipolar suction electrodes to functionally identify ipsilaterally-patched motoneurons. **B**: Whole-cell patch clamp recordings were performed in voltage clamp (VC; top trace) and current clamp (CC; bottom trace) modes from the same lL5 motoneuron in a sham preparation. Holding potential in VC mode is -60 mV, while cell membrane potential (V_m) in CC mode, without injecting any holding current, is -85 mV. **C**: Recordings were carried out in VC mode (top) and CC mode (bottom) from the same lL5 motoneuron after 90 minutes of BIKE. Holding potential in VC mode was -60 mV, while V_m in CC mode was -80 mV. Recordings from motoneurons in **B** and **C** were obtained from an equivalent period of time after isolation of the cord from the leg-attached preparation. Note the higher number of sPSCs (top trace in **C**) with respect to sham (top trace in **B**), as confirmed by the plot in **D**, reporting a significant increase in sPSCs frequency after BIKE-training (*; P = 0.001). **E**: In the graph are shown the I-V curves for sample motoneurons from BIKE and sham preparations. **F**: The plot indicates a significantly lower membrane

resistance (R_m) in BIKE-trained motoneurons with respect to sham (*; P = 0.04). **G** and **H**: Superimposed averaged traces represent fast sPSCs (**G**) and slow sPSCs (**H**) from a pair of sample motoneurons in sham (black lines) and BIKE-trained preparations (grey lines). **I** and **J:** Plots indicate that 90 minutes of BIKE increase frequency of fast sPCSs (**I**; *; P = 0.029), and slow sPCSs (**J**; *; P = 0.026), compared to sham experiments. In plots, grey dots represent raw data, bars indicate mean values.

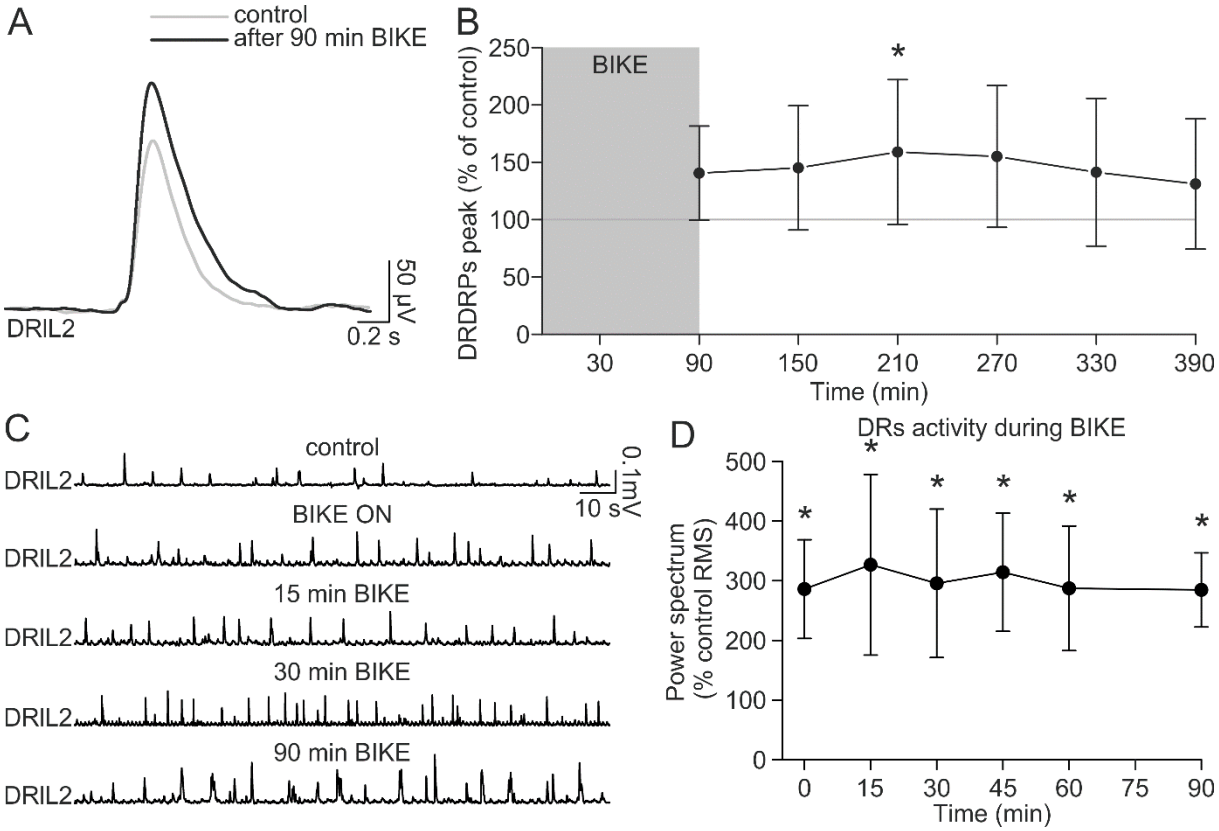

Figure 9. A 90-minute BIKE session stably increases DR reflexes and spontaneous discharges during training.

A: Averaged traces (mean of 5 sweeps) of DRDRPs were recorded from DRlL2 in response to electrical pulses applied to DRrL1 (rectangular pulses; duration = 0.1 ms; intensity = 80 µA, 4 x Th; frequency = 0.02 Hz) in pre-BIKE control (grey trace) and after a 90-minute BIKE session (black trace). **B**: The time course of DRDRP peaks recorded for up to five hours after BIKE (grey rectangle) highlights a significant increase in DRDRPs amplitude at two hours after training (*; P = 0.023). **C**: Spontaneous activity was recorded from DRlL2 in pre-BIKE control (top trace) and at different time points during BIKE training. **D**: The time course points out that magnitude of the power spectrum for spontaneous antidromic DR discharges was significantly increased as soon as BIKE was switched on and stably persisted throughout training duration (*; $P \leq 0.001$).

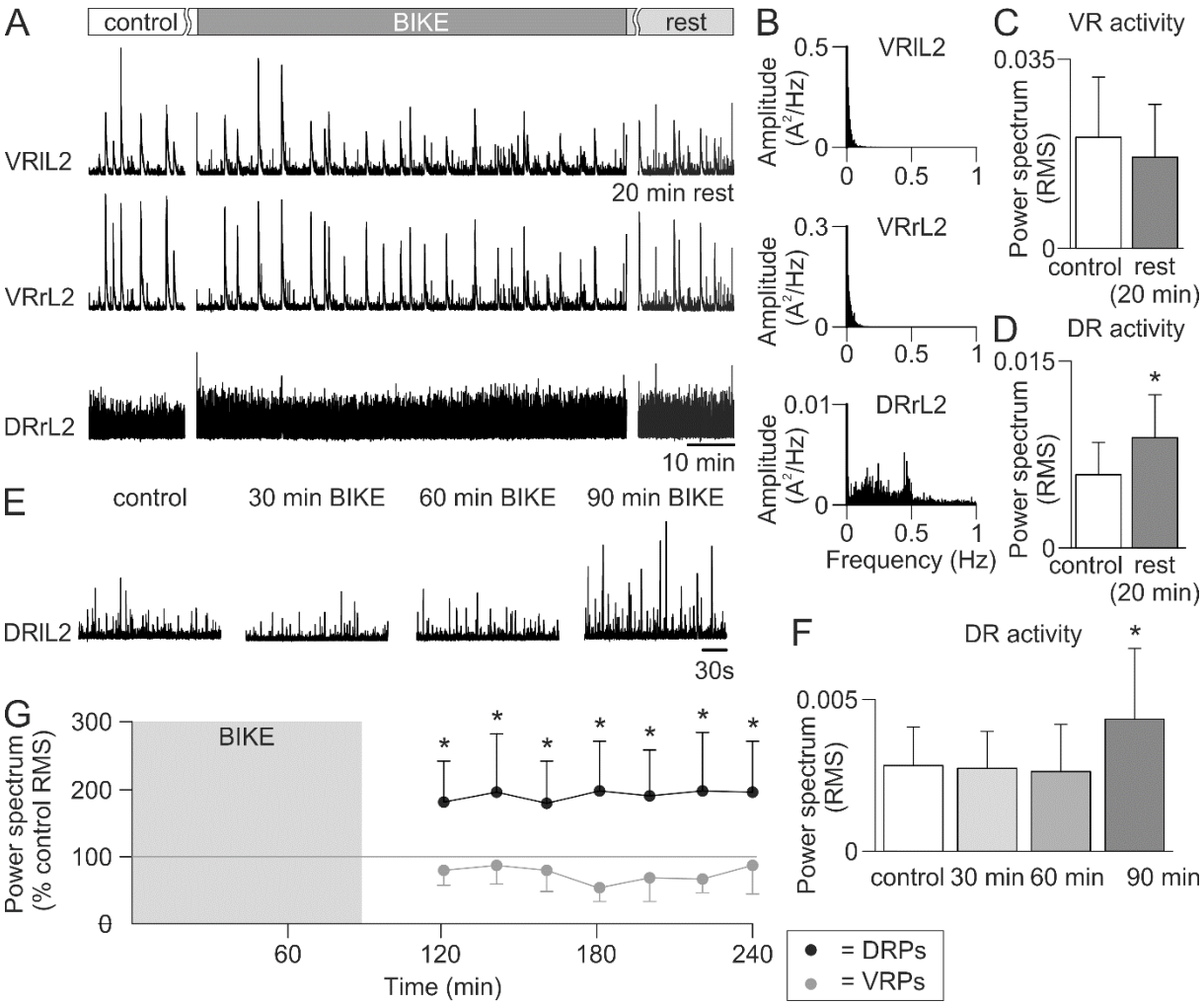

Figure 10. At least 90 minutes of BIKE are needed to increase spontaneous dorsal activity, which lasts throughout the following resting period.

A: As reported in the top bar, spontaneous activity was recorded from homosegmental L2 VRs and from DRrL2 in pre-BIKE control (left traces), during a 90-minute BIKE session (middle traces) and for the first 20 minutes of post-BIKE rest (right traces). Note that, during BIKE, VR activity did not change (middle, top traces; see also Fig. 5), while DR rhythm increased (middle, bottom trace; see also Fig. 9 C-D). Dorsal activity remained higher than pre-BIKE control also at the end of training (right, bottom trace). **B**: During BIKE functioning, power spectra of activity from bilateral VRs L2 (above panels) reveal the absence of any frequency component at 0.5 Hz, while rhythmic activity coupled with pedaling can be detected from DRrL2 (bottom panel). **C, D**: Histograms summarize average data of VR (**C**) and DR (**D**; *; $t_{(7)}$ = -4.058, P = 0.005) spontaneous discharges recorded after 20 minutes post-BIKE rest. **E**: Three subsequent sessions of BIKE (30 minutes each) were cumulatively applied, meanwhile spontaneous dorsal activity was recorded from DRlL2 at the

end of each session. Please note that the calibration bar on the right is the same for all traces in **E**. **F**: Bars show that only three consecutive 30-minute sessions of BIKE (for a total training period of 90 minutes) significantly increased DR rhythm magnitude (expressed as root mean square; RMS; *; $P = 0.026$), while a lower training duration was ineffective. **G**: The time course points out that after a 90-minute BIKE training (grey rectangle), DR spontaneous activity (black dots) remained higher than pre-BIKE control for at least two hours of post-BIKE rest (*; $P \leq 0.001$); on the other hand, VR spontaneous activity (grey dots) was unaffected by training. Spontaneous activity was assessed in 20-min bins, starting 10 minutes after the end of training.